Whole-limb scaling of muscle mass and force-generating capacity in amniotes

Peter J Bishop [Corresp., 1, 2], **Mark A Wright** [2], **Stephanie E Pierce** [2]

[1] Geosciences Program, Queensland Museum, Brisbane, Queensland, Australia

[2] Department of Organismic and Evolutionary Biology, Harvard University, Cambridge, Massachusetts, United States of America

Corresponding Author: Peter J Bishop
Email address: pbishop@fas.harvard.edu

Skeletal muscle mass, architecture and force-generating capacity are well known to scale with body size in animals, both throughout ontogeny and across species. Investigations of limb muscle scaling in terrestrial amniotes typically focus on individual muscles within select clades, but here this question was examined at the level of the whole limb across amniotes generally. In particular, the present study explored how muscle mass, force-generating capacity (measured by physiological cross-sectional area) and internal architecture (fascicle length) scales in the fore- and hindlimbs of extant mammals, non-avian saurians ('reptiles') and bipeds (birds and humans). Sixty species spanning almost five orders of magnitude in body mass were investigated, comprising previously published architectural data and new data obtained via dissections of the opossum *Didelphis virginiana* and the tegu lizard *Salvator merianae*. Phylogenetic generalized least squares was used to determine allometric scaling slopes (exponents) and intercepts, to assess whether patterns previously reported for individual muscles or functional groups were retained at the level of the whole limb, and to test whether mammals, reptiles and bipeds followed different allometric trajectories. In general, patterns of scaling observed in individual muscles were also observed in the whole limb. Reptiles generally have proportionately lower muscle mass and force-generating capacity compared to mammals, especially at larger body size, and bipeds exhibit strong to extreme positive allometry in the distal hindlimb. Remarkably, when muscle mass was accounted for in analyses of muscle force-generating capacity, reptiles, mammals and bipeds almost ubiquitously followed a single common scaling pattern, implying that differences in whole-limb force-generating capacity are principally driven by differences in muscle mass, not internal architecture. In addition to providing a novel perspective on skeletal muscle allometry in animals, the new dataset assembled was used to generate pan-amniote statistical relationships that can be used to predict muscle mass or force-generating capacity in extinct amniotes, helping to inform future reconstructions of musculoskeletal function in

the fossil record.

Whole-limb scaling of muscle mass and force-generating capacity in amniotes

Peter J. Bishop[1,2,*], Mark A. Wright[1] and Stephanie E. Pierce[1]

[1]Museum of Comparative Zoology and Department of Organismic and Evolutionary Biology, Harvard University, Cambridge, Massachusetts, USA

[2]Geosciences Program, Queensland Museum, Brisbane, Queensland, Australia

*Correspondence to: pbishop@fas.harvard.edu

Abstract

Skeletal muscle mass, architecture and force-generating capacity are well known to scale with body size in animals, both throughout ontogeny and across species. Investigations of limb muscle scaling in terrestrial amniotes typically focus on individual muscles within select clades, but here this question was examined at the level of the whole limb across amniotes generally. In particular, the present study explored how muscle mass, force-generating capacity (measured by physiological cross-sectional area) and internal architecture (fascicle length) scales in the fore- and hindlimbs of extant mammals, non-avian saurians ('reptiles') and bipeds (birds and humans). Sixty species spanning almost five orders of magnitude in body mass were investigated, comprising previously published architectural data and new data obtained via dissections of the opossum *Didelphis virginiana* and the tegu lizard *Salvator merianae*. Phylogenetic generalized least squares was used to determine allometric scaling slopes (exponents) and intercepts, to assess whether patterns previously reported for individual muscles or functional groups were retained at the level of the whole limb, and to test whether mammals, reptiles and bipeds followed different allometric trajectories. In general, patterns of scaling observed in individual muscles were also observed in the whole limb. Reptiles generally have proportionately lower muscle mass and force-generating capacity compared to mammals, especially at larger body size, and bipeds exhibit strong to extreme positive allometry in the distal hindlimb. Remarkably, when muscle mass was accounted for in analyses of muscle force-generating capacity, reptiles, mammals and bipeds almost ubiquitously followed a single common scaling pattern, implying that differences in whole-limb force-generating capacity are principally driven by differences in muscle mass, not internal architecture. In addition to providing a novel perspective on skeletal muscle allometry in animals, the new dataset assembled was used to generate pan-amniote statistical relationships that can be used to predict muscle mass or force-generating capacity in extinct amniotes, helping to inform future reconstructions of musculoskeletal function in the fossil record.

Introduction

Countless aspects of organismal biology vary with the size of the organism as a whole (Schmidt-Nielsen 1985; Vogel 2003). In a mechanical context, the differential scaling of lengths, areas, volumes, inertias and other metrics with increasing size (e.g., body mass) influences an organism's ability to generate and resist forces. An oft-cited example is the comparison between the cross-sectional area of a tissue and the gravitational loads it must bear. Under isometric (geometric) scaling, area scales proportional to length^2, or assuming a constant tissue density, mass$^{2/3}$; in contrast, gravity-induced loads scale proportional to mass^1. Thus, larger species would have disproportionately less tissue area to support their mass, incurring greater tissue stress (= force per unit area). Given that tissue mechanical properties are largely constant across species (e.g., yield strength of cortical bone; Currey 2002), this scaling relationship is undesirable, and usually necessitates changes to organismal structure, behaviour or performance to mitigate the effects of increasing body size, such as larger species using a more extended limb posture during stance and gait (Biewener 1989; Dick & Clemente 2017).

The macroscopic architecture of skeletal muscle is one such aspect of organismal structure that is known to scale with body size in animals. A particularly relevant architectural metric is its physiological cross-sectional area (PCSA), which relates a muscle's mass with the length and arrangement of its constituent fascicles (Calow & Alexander 1973; Gans & Bock 1965; Sacks & Roy 1982), and can be used to estimate the muscle's maximal force output in an isometric contraction (Powell et al. 1984; Medler 2002). If animals were isometrically scaled, muscle mass would scale in direct proportion to total body mass, fibre length would scale proportional to mass$^{1/3}$, and PCSA – and therefore force-producing capacity – would scale proportional to mass$^{2/3}$. Larger species would therefore be relatively weaker. Over the past five decades, numerous studies have examined the interspecific scaling of muscle mass and force-generating capacity (via PCSA) across a wide variety of species, in mammals (Alexander 1977; Alexander et al. 1981; Bennett & Taylor 1995; Cuff et al. 2016a; Cuff et al. 2016b; Eng et al. 2008; McGowan et al. 2008; Pollock & Shadwick 1994), birds (Bennett 1996; Maloiy et al. 1979) and non-avian saurians (Allen et al. 2015; Cieri et al. 2020; Dick & Clemente 2016). Although the caveat must be acknowledged that different studies have used different line-fitting approaches to

estimate scaling exponents, these studies have shown that across most species the architecture of individual muscles scales in a broadly similar fashion. Muscle mass typically exhibits weak negative to modest positive allometry (range of exponents 0.9–1.15), PCSA typically exhibits weak to modest positive allometry (range of exponents 0.69–0.91), and fascicle length typically exhibits modest positive to modest negative allometry (range of exponents 0.14–0.5). Some notable exceptions to this include the extreme positive allometry in the hindlimb extensors of macropod marsupials (mass exponents 1.11–1.61, PCSA exponents 0.78–1.33; Bennett & Taylor 1995; McGowan et al. 2008) and many forelimb muscles in varanid lizards (mass exponents 0.95–1.48, PCSA exponents 0.75–1.15; Cieri et al. 2020), and near mass independence of fascicle length in the plantaris of mammals (Pollock & Shadwick 1994; although this may be affected by sampling in that particular study). The common occurrence of positive allometry helps reduce the 'strength deficit' experienced by larger animals, but this deficit is fully counteracted only in extreme cases of positive allometry, where the PCSA exponent exceeds 1.

It remains unknown as to how the aforementioned scaling patterns for individual muscles translate to scaling at the level of the whole limb. Likewise, it remains unknown as to whether architectural disparities observed between muscles, functional groups of muscles (e.g., ankle extensors) or even species remain at the level of the whole limb. The limbs of an animal must exist and function as a single integrated entity, which imposes at least two requirements on the constituent muscles:

1. The muscles collectively share a common volume, whereby changes in the size of one muscle may affect the size of adjacent muscles (Fig. 1A). For example, in order for the limb to avoid becoming too heavy (or having too high a rotational inertia), increase in the size of one muscle may necessitate a decrease in the size of another.
2. Architectural specialization of muscles can limit their ability to effectively contribute to a diverse range of tasks (Wilson & Lichtwark 2011), and hence specialization in one muscle may necessitate concomitant change in another so that limb functionality is not compromised. For example, a muscle with short fascicles will have a high PCSA but a reduced working range, which may require another muscle to compensate by having longer fascicles, but with reduced PCSA (Fig. 1B).

These two requirements imply that animal limbs are subject to a 'fascicle packing problem', and raise the question of how flexible (evolutionarily labile) animal limbs are in terms of their muscular anatomy. Are there different strategies for packing PCSA into a given volume of limb muscle, or do the differences observed between individual muscles and between species 'cancel out' at the level of the whole limb? Depending on how stringent the above requirements are, the total force-producing capacity (strength) of an animal's limb may therefore be strongly tied to total limb muscle mass, irrespective of a given species' size or functional requirements.

Understanding how whole-limb muscle mass and force-generating capacity relate to one another, and how this relation scales with body size, is not just pertinent to the study of extant species. Muscle force-generating capacity is a key unknown in studies of extinct animal function and behaviour, and empirical data from extant species play a vital role in informing inferences of extinct species (Bates & Falkingham 2018; Bishop et al. 2021a; Fahn-Lai et al. 2020; Lautenschlager et al. 2018; Sellers et al. 2013). The use of empirical data from extant members of a specific clade may be appropriate for extinct members of that clade (e.g., using data derived from extant palaeognath birds to guide inferences of extinct palaeognath birds; Bishop 2015), but it is not immediately clear how this should be approached for extinct species that are phylogenetically distant or morphologically disparate from extant species. In particular, the more phylogenetically distant or morphologically disparate an extinct taxon is, the lower the confidence that can generally be placed in inferences of muscle origin or insertion (Carrano & Hutchinson 2002; Witmer 1995), relative size, internal architecture and even whether a given muscle exists in the extinct taxon (e.g., differentiation from adjacent muscles). Developing an understanding of how muscle mass and force-generating capacity scales with body size across a wide range of species, even at a broad anatomical resolution such as the whole limb, could therefore provide a useful starting point for better informed inferences of extinct taxa. Even if just overall bulk and strength of limb musculature were able to be confidently constrained, this would represent a practical advance upon which future refinements could be made.

The present study sought to address the above outstanding issues by conducting a holistic assessment of whole-limb muscle mass and force-generating capacity in extant terrestrial amniotes. It had three key aims: (1) to contribute new data from hitherto unsampled clades

(ameridelphian marsupials and lacertoid lizards), broadening the diversity of the available comparative dataset; (2) to investigate how muscles scale with body size at the level of the whole limb, in both the fore- and hindlimb, providing a first assessment of the stringency of the 'fascicle packing problem'; (3) to derive generic, amniote-wide statistical predictive relationships that would have utility in deriving inferences of musculature in extinct amniote species. This study is the first comparative synthesis of muscle architecture scaling across extant mammals, birds and non-avian saurians. In addition to providing a novel perspective on the topic of muscle scaling in animals, the results from this study provides a platform for more rigorous inference of muscle strength in extinct amniote clades.

Materials & Methods

Dataset

The present study is founded upon muscle architecture data derived from dissections (Table 1); all raw data used are provided in Table S1.The sources of the data are described in the following two subsections. Although this study addresses 'whole limb' scaling, it is restricted in scope to the musculature crossing the primary three joints of the limbs (shoulder/hip, elbow/knee and wrist/ankle), ignoring the intrinsic musculature of the manus and pes. This was necessitated by the practical difficulties of accurately dissecting and measuring the latter muscles (particularly for small species), such that data are very rarely reported in the comparative literature. Ignoring manual and pedal muscles is also justified given that they comprise a small fraction of total limb musculature, and presumably contribute only a small fraction towards limb support and propulsion during locomotor activities. Although extrinsic shoulder muscles attaching to the scapula can be important for locomotion in therian mammals (Hudson et al. 2011a; Jenkins & Weijs 1979), these were excluded from consideration to facilitate a fair comparison across all species; only muscles that explicitly attached to the humerus or more distal forelimb skeleton were included. The forelimb dataset comprised architectural measurements for a total of 912 muscles in 31 species (21 mammals and 10 non-avian saurians, the latter hereafter referred to as 'reptiles' for simplicity) spanning more than four orders of magnitude in body mass, and the

hindlimb dataset comprised measurements for a total of 1,181 muscles in 36 species (19 mammals, 12 reptiles and 5 birds) spanning almost five orders of magnitude in body mass. In the hindlimb dataset, birds and humans were collectively treated as a single group, 'bipeds', such that 'mammals' herein refer to all mammals except humans. Given the small sample size (and taxonomic skew) of birds in the current dataset, and the broad aims of the study, it was not considered justifiable to analyze birds and humans as separate entities here. Furthermore, as the present study concerns terrestrial amniotes, the forelimb of bipeds was not investigated.

For each muscle, its physiological cross-sectional area (PCSA) was calculated as

$$\mathrm{PCSA} = \frac{m_{\mathrm{muscle}} \cdot \cos(\alpha_{\mathrm{O}})}{\rho \cdot l_{\mathrm{O}}}, \quad (1)$$

where m_{muscle} is belly mass, α_{o} is pennation angle, ℓ_{o} is fascicle (or 'fibre') length and ρ is muscle tissue density, the latter taken to be constant for vertebrate skeletal muscle at 1,060 kg/m^3 (Hutchinson et al. 2015; Mendez & Keys 1960). It is important to note that this equation assumes that all fascicles of a muscle act in parallel in generating force, allowing their individual cross-sectional areas to be summed (see also Sacks & Roy 1982). In reality, the constituent fibres of a given fascicle are often shorter than the fascicle itself, wherein their ends overlap or interdigitate (Gaunt & Gans 1992; Infantolino et al. 2012), although they may still activate simultaneously with one another, thus functioning as a single fibre (Bodine et al. 1982). Additionally, as per common practice, it was assumed that measurements of fascicle length and pennation angle corresponded to the muscle's optimal fibre length and optimal pennation angle, respectively (Zajac 1989).

Published data

The majority of data used in this study were sourced from previously published comparative studies on muscle architecture, biomechanics or scaling (see Table 1 for references; see also Martin et al. 2020 for a review of methods used to measure muscle architecture). Unfortunately, many of the earlier studies on muscle architecture scaling cited in the Introduction did not report

their raw measurements and so their data were unable to be incorporated into a taxonomically richer analysis. Literature data were selected according to three requirements:

1. All or almost all of the muscles of the limb had been measured and reported (save the manual and pedal muscles, as noted above), since the overarching aim of the present study is considering the whole limb. Studies in which a few small muscles (e.g., deep muscles such as the gemellus, quadratus femoris or popliteus) were not reported were still included, since the omission of such small muscles is expected to have minimal effect on the overall results. Studies that measured multiple muscles under a single name (e.g., multiple heads of the flexor carpi radialis as a single muscle) were also included, since this nevertheless accounts for all the muscle mass present. In contrast, studies that did not report one or more major muscles were excluded from consideration. All datasets ultimately selected for use in the present study included all major extensor and adductor (antigravity) muscles of the limb. The specific muscles included (and which, if any, were excluded) in a given source study are outlined in Table S1.
2. Each of the architectural parameters listed in Equation 1 were either explicitly reported, or their values able to be back-calculated from reported values, the latter either as PCSA (e.g., Cuff et al. 2016a,b; back-calculated via Equation 1) or mass-scaled values (e.g., Dick and Clemente 2017, Cieri et al. 2020; back-calculated by unscaling according to reported body mass). A few previous studies had neglected to measure (or at least report) pennation angle, but to maximize consistency across the present dataset these studies were excluded. Studies that reported dry muscle mass only were also excluded.
3. The data reported were for adult or large-sized individuals, to reduce potential confounding effects of ontogenetic variation (Table S1). In approximately two-fifths of species sampled, multiple similarly-sized individuals had been investigated, but the data reported by the relevant studies were only presented as a species mean, wherein a given architectural parameter for a given muscle had already been averaged across the individuals studied; in these cases, the mean body mass of that sample was used. For all other species, architectural and body mass data were reported for separate individuals. When data for multiple individuals of a given species had been reported separately (e.g., Lamas et al. 2014, Allen et al. 2015, Martin et al. 2019), those for the largest individual were used, to reduce possible ontogenetic effects. This approach was deemed more appropriate than computing a species

average across all individuals, because in several instances the sample of individuals investigated by prior studies (especially those focused on ontogeny) exhibited high disparity in body sizes, undermining the value of a species mean; moreover, such an arithmetic mean would not account for ontogenetic allometry within the species, and hence could introduce further error into the analyses. Ultimately, each species contributed only a single datapoint to the analyses.

Data were also sourced for a further 15 species from six additional studies, which had reported just muscle mass (Table S1). These studies either reported mass of each individual muscle separately (Hudson et al. 2011a; Hudson et al. 2011b; Ogihara et al. 2009; Payne et al. 2006; Zihlman et al. 2011), or reported total muscle mass for the limb as a whole (Grand 1977), and helped further increase taxonomic coverage in the final dataset.

New data

To broaden the taxonomic diversity of the dataset, and contribute novel data that future studies may draw upon, dissections were undertaken on a single adult individual each of the Virginia opossum (*Didelphis viginiana*) and the Argentine black and white tegu (*Salvator merianae*). The former is an ameridelphian marsupial, and apart from a single species of bandicoot (australidelphian; Martin et al., 2019) is the only other marsupial in the dataset; the latter is a lacertoid lizard, representing a hitherto unsampled part of squamate phylogeny. Intact whole carcasses of wild individuals were obtained as part of a prior study (Fahn-Lai et al. 2020), sourced from Worcester County, Massachusetts (*D. virginiana*, Massachusetts Division of Fisheries and Wildlife) and Everglades National Park, Florida (*S. merianae*, Daniel Beard Center, United States Geological Survey). Upon acquisition, the specimens were immediately frozen at -20°C, and subsequently fully thawed prior to dissection and architectural measurement. The right fore- and hindlimbs were dissected in both cases. Muscle architecture measurement followed standard dissection procedures (Allen et al. 2015; Biewener & Full 1992; Fahn-Lai et al. 2020), using a magnifying lamp where necessary. To minimize desiccation of the fresh specimens, tissues were kept moistened with paper towel soaked in saline solution throughout. Muscle belly mass was measured with an electronic balance (Precisa 320 XB,

Precisa Gravimetrics AG, Dietikon; 0.0001 g precision), fascicle length with digital calipers (0.01 mm precision) and pennation angle with a transparent protractor (1° precision). Measurements of fascicle lengths and pennation angles were made at random locations throughout a muscle belly, and depending on muscle size up to ten measures each were made, after which the arithmetic mean was derived.

Anatomical comparisons

Four main, and two subsidiary, comparisons were undertaken for both fore- and hindlimbs, as described below. For each comparison, patterns were examined for the limb as a whole, as well as just the proximal and distal limb muscles separately, given that some previous studies have noted scaling differences between the proximal and distal limb for individual muscles or functional groups (Alexander et al. 1981; Cuff et al. 2016a; Cuff et al. 2016b; Dick & Clemente 2016; Eng et al. 2008). 'Proximal' muscles were classified as those in which the majority of their bulk resides proximal to the elbow (forelimb) or knee (hindlimb) joints, whereas 'distal' muscles have the majority of their bulk residing distal to those joints. This volume-based approach is more relevant to the 'fascicle packing problem', and avoids the complications caused by flexor or extensor muscles crossing the joints involved. Furthermore, given that a substantial component of hindlimb locomotor muscle in reptiles is the caudofemoralis longus (CFL), which chiefly resides in the proximal tail, whole hindlimb and proximal hindlimb analyses were also re-run with this muscle excluded from the reptile sample. In addition to providing more nuanced insight into questions of scaling and fascicle packing, these additional variations provide greater sophistication to predictive relationships derived from the data. Ultimately, eight different sub-analyses were performed for each anatomical comparison (48 in total).

#1 – Total muscle mass (Σm_{muscle}) v. body mass (m_{body})

This comparison examines how much of total biomass is invested in limb musculature; under isometry, the scaling exponent would be 1. It ignores the potential for systematic variation in relative body composition in terms of other tissue types (bone, integument, etc.), but is

nonetheless informative because it focuses on one of the tissues primarily involved in body support and propulsion during terrestrial locomotion.

#2 – Mean size-normalized isometric strength v. m_{body}

Following calculation of PCSA as per Equation 1, the arithmetic mean across all muscles was taken. Although PCSA is an estimator of maximal isometric force-generating capacity of a muscle, as a measure of area it is not a particularly intuitive descriptor of force, in and of itself. To present mean PCSA in a more tangible form, it was converted to maximal isometric force in multiples of body weight (BW):

$$F_{max}* = \frac{\text{PCSA} \cdot \sigma}{m_{body} \cdot g}, \quad (2)$$

where σ is maximal isometric stress, assumed here as 300,000 N/m^2 (Bates & Falkingham 2018; Hutchinson 2004; Medler 2002), and g is the acceleration due to gravity. Dividing by body mass means that under isometry the scaling exponent is that of PCSA minus 1.0 (i.e., -⅓), which in turn makes it more straightforward to interpret in the context of scaling. That is, PCSA can scale with positive allometry and yet force-generating capacity can decline with increasing size if ⅔ < PCSA exponent < 1, whereas the sign of the exponent for F_{max}* is immediately indicative of whether a strength deficit exists at larger body size: only if it is positive is relative force-generating capacity (i.e., relative performance) maintained with increasing size. It should be noted that using a different value for σ would not alter the resulting scaling exponent.

#2b – Median F_{max}* v. m_{body}

The relative masses and force-generating capacities of individual limb muscles typically do not follow an even or symmetrical distribution (Table S1), such that the analysis of means as above may be influenced by one or two exceedingly strong, or weak, muscles in the limb. Thus, the median PCSA for all muscles was also computed, and converted to F_{max}* as per Equation 2. Under isometry, the scaling exponent would also be -⅓.

#2c – Total F_{max}* v. m_{body}

In the current dataset there is considerable variation in the number of individually measured and reported muscles for a given species. These differences can reflect investigator judgement in the splitting or grouping of muscle heads for measurement, but can also be due to legitimate anatomical differences between species; for example, crocodylians have a single long digital flexor in the hindlimb, whereas birds have up to six. Variation in the number of muscles may influence the mean or median PCSA, and so to account for this the total PCSA was also computed and converted to F_{max}* as per Equation 2. Again, under isometry the scaling exponent would be -⅓.

#3 – Characteristic fascicle length v. m_{body}

Fascicle length is almost ubiquitously investigated in studies of muscle architecture scaling, yet in a broad comparison across amniotes it is not sensible to investigate fascicle length in and of itself, either for individual muscles, functional groups or for the whole limb. This is due to the great variation that can exist in muscle size, origins, insertions and lengths, as well as differences of subdivision (differentiation) between different taxonomic groups, which can all lead to marked variation in fascicle length irrespective of body size. An alternative approach is to compute a single 'characteristic fascicle length' for the limb as a whole, as the weighted harmonic mean of the fascicle lengths of each individual muscle (cf. Alexander et al. 1981):

$$L^* = \frac{\Sigma m_{muscle}}{\rho \cdot \Sigma PCSA}. \quad (3)$$

This effectively replaces the musculature of the whole limb (or proximal or distal compartment thereof) with a single equivalent muscle. Note that in using PCSA, Equation 3 weights fascicle lengths by both muscle mass and $\cos(\alpha_o)$, and thus the equivalent whole-limb muscle also factors in pennation. Furthermore, it can be seen that L^* is approximately inversely proportional to mean relative (mass-normalized) PCSA (Eng et al. 2008). As for 'real' fascicle length, the scaling exponent under isometry would be ⅓.

#4 – ΣPCSA v. Σm_{muscle}

By removing the context of m_{body}, this provides a direct assessment of the 'fascicle packing problem', by testing how whole-limb force-generating capacity compares against the amount of available muscle mass. Under isometry, the scaling exponent would be ⅔; note that isometry may reflect scale invariance of pennation angle (which would be theoretically expected; see also Dick and Clemente 2017, Cieri et al. 2020), fascicle length, or a more complex combination of both parameters. Comparison 3 also addresses the fascicle packing problem, but indirectly.

Statistical analyses

All data processing and analyses were conducted in R v.4.1.0 (R Core Team 2021), using the 'caper' (v.1.0.1; Orme et al. 2018), 'evomap' (v 0.0.9; Smaers & Rohlf 2016) 'phytools' (v.0.7; Revell 2012), 'geiger' (v.2.0.7; Harmon et al. 2008) and 'nlme' (v. 3.1; Pinheiro et al. 2021) packages; the full set of code and data used are provided in the Supplemental Information. Data were logarithmically transformed (base 10) prior to analysis, facilitating the use of linear statistical models. Phylogenetically informed statistical analyses were conducted using a single, fully resolved, time-calibrated phylogenetic tree of the study taxa (Fig. S1). The tree was generated using the TimeTree database (www.timetree.org; Hedges et al. 2006), which included all taxa except for *Isoodon fusciventer*; this was substituted with *Isoodon obesulus* (the only species of *Isoodon* in the database), which has no effect on divergence times with respect to other taxa in the present study.

For each of the above anatomical comparisons (for whole-limb and proximal and distal compartments), allometric scaling equations of the form $\log_{10}Y = \log_{10}A + B\log_{10}X$ were derived for mammals, reptiles and bipeds separately, using phylogenetic generalized least squares (pGLS or 'phylogenetic regression'; Smaers & Rohlf 2016) to determine slopes (exponents, B) and intercepts ($\log_{10}A$). This simultaneously estimated the λ parameter of Pagel (1999) using maximum likelihood, offering greater flexibility than a strict Brownian motion model of evolution in accounting for phylogenetic signal in the data. Additionally, the 95% confidence interval (CI) of the slope was determined, using the t-distribution, to facilitate comparison against the slope expected under isometry: if the expected exponent fell outside of the CI, the

scaling was deemed to significantly depart from isometry at the $P = 0.05$ level. Subsequently, all groups were collated together and a new pGLS fit was computed to generate a 'pan-amniote' regression for a given anatomical comparison (again for whole-limb and proximal and distal compartments), thus deriving a statistical predictive framework that can be applied to extinct species. In addition to estimator coefficients, 95% CIs and prediction intervals were also derived (Smaers & Rohlf 2016), which can provide error margins for future estimations.

To ascertain whether mammals, reptiles or bipeds exhibited different allometric trajectories for a given anatomical comparison, a phylogenetic analysis of covariance (pANCOVA) was performed, which tested for differences in slope and intercept between groups (both separately and together; Smaers & Rohlf 2016). Here the off-diagonal elements of the variance–covariance matrix were scaled by the λ parameter estimated during calculation of the pan-amniote regression, to minimize false negatives caused by an overly conservative assumption of strict Brownian motion. The analyses were also run without accounting for phylogeny (ANCOVA, $\lambda = 0$), to evaluate the effect of phylogenetic relatedness on the results, given that the mammal, reptile and biped samples are nearly mutually exclusive phylogenetically. Statistical significance was set at $P = 0.05$.

Results

Scaling results and exponents are presented graphically in Figs 2–5; as the results for mean F_{max}* (comparison 2) were highly similar to those for median and total F_{max}* (comparisons 2b and 2c, respectively), the latter are presented in the Supplemental Information (SI text, Figs S2, 3). The results for hindlimb analyses excluding the caudofemoralis longus (CFL) from the reptile (i.e., non-avian saurian) dataset are presented in Figs S4–S9. The results of inter-group comparisons of allometries are presented in Tables 2–5, with those for median and total F_{max}* presented in the Supplemental Information (Tables S2, 3); the results for hindlimb analyses excluding the CFL from the reptile dataset are presented in Tables S4–S9. Coefficients for the pan-amniote regressions are reported in Table 6, with coefficients for hindlimb analyses excluding the CFL from the reptile dataset presented in Table S10.

429
430
431 **Total muscle mass v. body mass**
432
433 Reptiles almost ubiquitously show negative allometry, whereas mammals and bipeds do not
434 show significant departure from isometry (Fig. 2). The one exception to this generalization is
435 negative allometry in the distal hindlimb of mammals: larger mammals tend to have relatively
436 lighter (less muscled) distal hindlimbs. When the CFL is excluded, the values of the slopes (and
437 CIs) for reptiles change minimally, but this is sufficient to render the revised scaling statistically
438 indistinguishable from isometry (Fig. S4). Analyses of covariance (without accounting for
439 phylogeny) indicate that mammals, reptiles and bipeds each exhibit significantly different
440 allometric trajectories, in terms of both slope and intercept (Tables 2, S4). Reptiles have a lower
441 slope and intercept compared to mammals, indicating that they have proportionately lower
442 muscle mass, especially at large body sizes. In contrast, bipeds have proportionately greater
443 hindlimb muscle mass than both mammals and reptiles, especially at larger body size and
444 particularly in the distal limb. Many of these differences disappear (i.e., become statistically non-
445 significant) once phylogeny is taken into consideration using the pANCOVA
446
447
448 **Mean size-normalized isometric strength (F_{max}*) v. body mass**
449
450 Both mammals and reptiles generally do not show significant departure from isometry, although
451 reptiles exhibit negative allometry in the distal hindlimb (Fig. 3). When the CFL is excluded, the
452 values of the slopes for reptiles change minimally, but narrower CIs render the revised scaling
453 significantly negatively allometric, for both the whole and proximal hindlimb (Fig. S5). Notably,
454 bipeds exhibit strong positive allometry throughout the hindlimb, particularly in the distal limb
455 (Fig. 3); notwithstanding the small sample size, mean size-normalized force-generating capacity
456 appears to be scale-invariant. Analyses of covariance without accounting for phylogeny indicate
457 that mammals, reptiles and bipeds frequently exhibit significantly different allometric
458 trajectories, especially in terms of slope (Tables 3, S5). Differences in intercept were mostly
459 detected for the forelimb, where reptiles exhibit a markedly lower intercept than mammals,

indicating lower mean force-generating capacity regardless of body size. Most of the differences between mammals and reptiles disappear once phylogeny is taken into consideration using pANCOVA; in contrast, most differences between mammals and bipeds, and reptiles and bipeds, were retained following phylogenetic correction, attesting to strong allometric deviation in the biped sample.

Characteristic fascicle length (*L) v. body mass**

In the forelimb, both mammals and reptiles exhibit negative allometry, although in reptiles this is not statistically significant in the distal limb, due to wide CIs in that instance (Fig. 4). Mammals and bipeds also exhibit negative allometry in the hindlimb, although in mammals this is driven by the distal limb only; mirroring patterns noted above, bipeds show a stronger departure from isometric scaling in the distal limb. Reptiles do not show any significant departure from isometry in the hindlimb, a result that remains unaltered when the CFL is excluded from the dataset (Fig. S8). In stark contrast to the previous comparisons, ANCOVA (without accounting for phylogeny) revealed almost no significant difference among mammals, reptiles or bipeds (Tables 4, S8). The only difference detected (which disappeared following phylogenetic correction using pANCOVA) was that mammals have a lower intercept in the distal hindlimb compared to both reptiles and bipeds, indicating that, overall, the distal hindlimb of mammals possesses proportionately shorter muscle fascicles.

Total PCSA v. total muscle mass

Mammals and bipeds almost ubiquitously exhibit positive allometry, whereas reptiles generally do not exhibit statistically significant departures from isometry (Fig. 5). Two exceptions to this are mammals not showing a significant departure from isometry in the distal forelimb, and reptiles exhibiting positive allometry in the forelimb as a whole. Excluding the CFL does not significantly alter the reptile hindlimb scaling patterns (Fig. S9). As for *L**, ANCOVA (without accounting for phylogeny) notably revealed almost no significant difference among mammals,

reptiles or bipeds (Tables 5, S9). Mammals have a lower slope in the hindlimb overall compared to bipeds, although this cannot be attributed to differences within the proximal or distal compartments. Additionally, mammals have a higher intercept in the distal hindlimb compared to reptiles (a result which disappeared following phylogenetic correction using pANCOVA), indicating that the distal limb of mammals possesses relatively greater fascicle area.

Pan-amniote regression

Coefficients for the pan-amniote regressions (Table 6) provide an empirical basis for estimating some important measures of muscle mass and force-generating capacity in extinct terrestrial amniotes. Note that the coefficients reported here were computed to the exclusion of bipeds, given that bipeds have been shown above to frequently differ from quadrupeds, and that the majority of species throughout tetrapod history were quadrupedal. The code provided in the Supplemental Information enables for predictive relationships to be derived that includes bipeds in the dataset. In addition to the coefficients, mean percent prediction error (%PE) is also reported, expressed in terms of the original, non-log-transformed dimensions of the data (Smith 1980); this provides an alternative to prediction intervals (see SI code) as a way of deriving upper and lower estimates for a given taxon. Coefficients computed when the CFL was excluded from the reptile dataset (Table S10) are largely similar to those reported in Table 8, although notably mean %PE is generally higher.

Discussion

Through a synthesis of new dissection data with previously published results, the present study aimed to holistically appraise limb muscle scaling in terrestrial amniotes. In particular, it sought to investigate how muscle mass (size) and force-generating capacity (strength) scales at the level of the whole limb, to explore whether this reflects previously observed patterns noted for individual muscles or functional groups across disparate clades, and to assess how tightly constrained amniote limbs are in terms of whole-limb muscular composition. A subsidiary

objective was to generate statistical relationships that have predictive value in inferring function in extinct amniotes. In synthesizing data from numerous studies, it must be acknowledged that the resulting dataset will likely contain a certain level of 'noise' due to various sources. One pertinent source of error is the measurement of fascicle length in fresh specimens: as was the case in the present study, this is typically undertaken following removal of a given muscle from the limb, whereupon the fascicles may non-systematically deviate from a 'reasonable' or functionally relevant length. This problem may be partially mitigated by using formalin-fixed specimens, where the limb joints can be locked in physiologically realistic poses prior to fixation (thus limiting fascicle length change after the muscle is removed), although this approach can involve its own set of challenges, such as muscle shrinkage (Martin et al. 2020; Kikuchi and Kuraoka 2014). Digital methods that permit architectural measurement *in situ*, such as contrast-enhanced scanning and automated fascicle tracking (e.g., Sullivan et al. 2019), may be able to avoid these issues, but thus far are limited in spatial scale and hence anatomical and taxonomic scope. Additional sources of noise in the present study will also include variation in the approaches of prior studies, in terms of investigator, occasional exclusion of some small muscles, subjective subdivision of muscle complexes and so on. Nonetheless, given the wide diversity and size range of species covered here, this was considered acceptable for the present study's broad scope.

Mass and force-generating capacity scaling across terrestrial amniotes

In terms of total muscle mass (Fig. 2), the present study found that reptile (i.e., non-avian saurian) limbs typically show negative allometry with respect to body mass (exponents 0.884 to 0.939), whereas mammals (exponents 0.989 to 1.019) and bipeds (exponents 1.104 to 1.109, but wide CIs) typically displayed isometry. This is in partial agreement with prior studies, where weak negative to modest positive allometry has been recovered (exponents 0.9 to 1.15 across all amniotes; see references in Introduction). The differences in findings may be due to multiple factors, including variation in sample sizes affecting CI calculation, the line-fitting approach used and even the species that contribute to the underlying datasets. It may also reflect a genuine biological phenomenon, where allometric patterns observed for a select few muscles (i.e., those

553 which extend the range of exponents recovered by previous studies) are 'cancelled out' by those
554 of many other muscles, when considered together at the level of the whole limb. Irrespective of
555 the proximate cause(s), it is evident that reptiles have proportionately less muscle mass than
556 mammals or bipeds, and bipeds have proportionately greater hindlimb muscle mass, especially in
557 the distal limb. Neither result is hardly surprising, given that the reptiles sampled have short
558 limbs and a long, massive tail that contributes substantially toward total body mass, and that
559 bipeds (by virtue of being bipeds) ought to invest a greater fraction of body mass into longer,
560 more heavily muscled hindlimbs.
561
562 Muscle force-generating capacity in the present study was expressed in a more intuitive fashion
563 by normalizing to units of body weight. Thus, to compare exponents derived here to those of
564 prior studies that have examined PCSA directly, this requires adding or subtracting 1.0 to the
565 exponent. Three different measures of normalized force-generating capacity (F_{max}*) were
566 explored here – mean (Fig. 3), median (Fig. S2) and total (Fig. S3) – which showed a consistent
567 overarching set of patterns with respect to body mass. Mammals and reptiles overall exhibit
568 isometric scaling, although in some circumstances mammals tended towards positive allometry
569 (total range of exponents -0.30 to -0.245) whereas reptiles tended towards negative allometry
570 (total range of exponents -0.465 to -0.302). This is partially consistent with the results of prior
571 studies (corrected exponents -0.31 to -0.09; see references in Introduction). Again, discrepancies
572 in findings may belie the different spatial scales concerned; for example, the high end of
573 previously reported exponents derive from the plantaris muscle of the mammalian hindlimb
574 (Pollock & Shadwick 1994) and the proximal forelimb of felids (Cuff et al. 2016a). Of note,
575 reptiles often displayed a markedly lower intercept than mammals or bipeds, indicative of
576 reduced relative force-generating capacity and again consistent with possessing short limbs and
577 massive tails. It therefore follows that how 'body mass' is gauged (total body mass, body mass
578 excluding tail, etc.) will influence interpretations of interspecific differences in force-generating
579 capacity, although from a purely mechanical perspective total body mass is appropriate in the
580 context of terrestrial locomotion, since ultimately the limbs must support and propel all of it.
581
582 Bipeds were found to almost ubiquitously display positive allometry in muscle force-generating
583 capacity, and were frequently found to significantly differ from mammals and reptiles even after

584 phylogeny was accounted for (in 13 of 15 comparisons with mammals, all comparisons with
585 reptiles); again, this can be related to the greater investment of biomass in the hindlimbs of these
586 species. Notably, positive allometry was exceedingly strong in the distal hindlimb (total range of
587 exponents -0.016 to 0.025), to the point that relative force-generating ability may *increase* with
588 increasing body size. This is comparable to exponents reported for bipedal hopping macropods
589 (corrected exponents -0.22 to 0.33; Bennett & Taylor 1995; McGowan et al. 2008), although
590 intriguingly is higher than the exponents recovered by Maloiy et al. (1979) for the ankle
591 extensors of a selection of ground-dwelling birds (corrected exponent -0.24 to -0.19). These
592 results should be viewed with some caution, given that only six species were examined in the
593 present study. Nonetheless, they raise the interesting question of whether extreme positive
594 allometry would persist at larger body sizes beyond the largest extant biped, the ostrich (*Struthio*
595 *camelus*). For example, how would muscle strength fare in multi-tonne non-avian theropod
596 dinosaurs, and what implications may this have for locomotor performance? These are questions
597 that must await future investigation, but the comparative dataset marshalled here can provide an
598 empirical basis for such efforts.
599
600 In lieu of investigating fascicle length *per se*, this study examined an equivalent region-level
601 metric, characteristic fascicle length (L^*), which tended to exhibit negative allometry with
602 respect to body mass in both mammals and bipeds, as well as the forelimb of reptiles. The
603 exponents obtained (0.171 to 0.324) fell within the range reported previously for actual fascicle
604 length in individual muscles or functional groups (0.14 to 0.5; see references in Introduction).
605 Negative allometry indicates that muscle fascicles are on the whole proportionately shorter in
606 larger species. This is especially true in the mammalian distal hindlimb, which also exhibits a
607 lower intercept (Fig. 4); shorter muscle fascicles in the distal hindlimb of mammals in turn
608 translate to relatively greater PCSA per unit mass in this compartment (Fig. 5). All else being
609 equal, proportionately shorter muscle fascicles in larger species will translate to reduced joint
610 excursion, and at least for mammals and birds this correlates with the habitual use of more
611 extended limb postures in larger species (Biewener 1989; Biewener 2005; Bishop et al. 2018;
612 Gatesy & Biewener 1991).
613
614

615

616 ***Fascicle packing***

617

618 Analysis of covariance of muscle mass and force-generating capacity identified numerous
619 differences in scaling patterns between mammals, reptiles and bipeds, but when phylogeny was
620 taken into account the majority of these became statistically non-significant (Tables 2 ,3, S2, S3).
621 Hence there are genuine physical differences in mass or force-generating capacity between each
622 group (which is biomechanically relevant), and these largely exist due to each group having
623 evolved along different phylogenetic trajectories. However, when total muscle mass was factored
624 into consideration, either directly (comparison 4: ΣPCSA v. Σm_{muscle}) or indirectly (comparison
625 3: L^* v. m_{body}, wherein Σm_{muscle} is used to compute L^*), ANCOVA recovered almost no
626 statistically significant difference between any group; this was true regardless of whether
627 phylogeny was accounted for or not, and was observed for the limb as a whole as well as
628 proximal and distal compartments separately (Tables 4, 5). That is, the fore- and hindlimbs of
629 reptiles, mammals and bipeds almost ubiquitously follow a single common scaling pattern[1]. This
630 in turn implies that observed differences in whole-limb force-generating capacity between
631 groups are principally driven by differences in limb muscle mass, not internal architecture: one
632 group does not 'pack their fascicles better' for a given volume of limb muscle, they just invest a
633 greater fraction of total biomass into limb muscle in the first instance. The only possible
634 exception to this generality is the distal hindlimb of mammals, which at larger body sizes at least
635 do indeed appear to 'pack their fascicles better', with a greater PCSA (and in turn, force-
636 generating capacity) per unit muscle mass, correlating with proportionately shorter fascicles for a
637 given body size. All else being equal, this result suggests that larger species may benefit from
638 greater elastic energy storage in the distal hindlimb tendons during locomotion (cf. Pollock &
639 Shadwick 1994), although it should nevertheless be treated with caution, since a large proportion
640 of the currently sampled mammals are 'cursorial' taxa, which may bias the analysis.

641

[1]This might at first seem at odds with the finding that, for example, mammals exhibit positive allometry whereas reptiles do not show a significant departure from isometry. The apparent contradiction can be reconciled by noting that these comparisons are testing two different things in isolation of one another, whereas in reality there is a gradation across successively overlapping exponents and CIs – the statistical analogue of a 'ring species'.

The existence of a single overarching pattern, across a diverse array of terrestrial amniotes that span more than four orders of magnitude in body mass, is remarkable. It implies the tendency towards some adaptive optimum in organismal 'design' or, more likely, the presence of one or more constraints that prevent significant and systematic deviation from a common pattern. These constraints may be functional in nature, such as trade-offs that could occur between conflicting requirements of individual muscles in the execution of disparate tasks (see Introduction), or may have a developmental basis (e.g., Evans et al. 2021). Given the multidimensional and nonlinear aspects of muscle architecture and function, and terrestrial locomotor biomechanics in general, it would be naïve to suggest that a bivariate statistical model such as those derived here can sufficiently represent the mechanical phenomena involved (Taylor & Thomas 2014). Deciphering the proximate underlying cause(s) of this strong consistency must therefore await future study. It is also important to recognize that there is still scope for (non-systematic) variation; for example, the greyhound (*Canis familiaris*, 27 kg) and snow leopard (*Panthera uncia*, 36 kg) have near-identical total hindlimb muscle mass (~1.64 kg), yet the greyhound – which is selectively bred for high-speed running – has approximately double the PCSA of the snow leopard (0.028 v. 0.014 m^2; Table S1). Important insight into the fascicle packing problem can therefore be gained by better understanding the reasons for variation about the common pan-amniote pattern, through exploring variables that were not investigated in the current analyses, such as segment lengths, muscle moment arms, joint mobility, posture and locomotor ecology.

Considerations for future studies

A number of other points are worth noting in the context of future comparative investigations of muscle architecture. Firstly, despite a superficially broad taxonomic coverage, the dataset of the present study is still biased, with few birds, marsupials or non-varanid squamates, numerous 'cursorial' eutherians and not one testudine; future studies should therefore target currently under- or unsampled parts of amniote phylogeny. Increased diversity will be especially useful for elucidating the true extent, and underlying cause(s) of, conservatism in whole-limb fascicle packing. Furthermore, it is recommended that as much architectural data be collected and reported as possible, even if it may not all be immediately used in a given study, since this will

maximize its potential utility for later studies. One reason why several prior datasets were excluded from the present study was their omission of pennation angle from the set of reported (or even collected) measurements. A second point worth considering is that, out of necessity, the present study ignored the intrinsic musculature of the manus and pes; if further datasets for these muscles become available in the future, they should be analysed, since this may reveal important differences between plantigrade and digitigrade species.

One final consideration is that the present study found numerous differences between mammals, reptiles and bipeds in the allometry of muscle mass and force-generating capacity with respect to body mass. This is hardly surprising, but it has an important implication for how comparative studies should undertake their analyses. In order to facilitate comparison within or across species, previous studies that have explored muscle architecture and function typically normalize raw architectural measurements by body mass, or the dimensionally appropriate exponent of body mass such as $m_{body}^{1/3}$ for normalized fascicle length (Allen et al. 2010; Bates & Schachner 2012; Dick & Clemente 2016; Fahn-Lai et al. 2020; Martin et al. 2019; Regnault et al. 2020). This may be acceptable for comparisons of closely related species, but becomes questionable when divergent allometries with body mass are involved. A more sensible approach for future studies would be to normalize against more directly relevant parameters, such as limb or limb segment length, or alternatively by the appropriate clade-specific scaling exponents. Exactly which is the most appropriate normalizing metric to use may vary depending on a given study's core questions, and deserves further scrutiny.

Conclusion

Whole-limb scaling of muscle mass and force-generating capacity generally follows the same patterns reported previously for individual muscles or functional groups of muscles, although some instances of tendency towards isometry (as opposed to previously reported positive or negative allometry) were noted. This is the first time that muscle scaling has been addressed at such a broad spatial scale, across a diverse array of terrestrial amniotes. Additionally, some important differences were observed between proximal and distal limb compartments,

particularly in the hindlimb of mammals and bipeds, which may reflect the 'cursorial' habits of many of the species investigated here. The mammalian distal hindlimb has proportionately less muscle mass and shorter fascicles, but per unit muscle mass has a higher PCSA; and the distal hindlimb of bipeds has proportionately greater muscle mass and PCSA.

Almost all differences in force-generating capacity between groups appear to be due principally to differences in muscle mass, rather than muscle architecture. Thus, one group does not systematically 'pack their fascicles better' than another, instead they simply invest more biomass into limb muscle. The underlying reason(s) for a single overarching relationship across extant amniotes remains to be determined, although it echoes conservatism in other aspects of musculoskeletal design, such as tissue mechanical properties.

A comparative dataset of extant amniotes spanning almost five orders of magnitude in body size has been assembled, which can be built upon and used by future studies in the analysis of muscle architecture diversity. This dataset also forms the basis for a suite of pan-amniote predictive equations that can be used to estimate bulk muscle mass and force-generating capacity, along with error margins, for extinct species. These can be used if estimates of body mass are available, or alternatively from estimates of total limb muscle volume, as derived from digital volumetric reconstructions based on skeletal material. Reliably inferring the force-generating capacity of individual muscles in extinct species remains elusive (Bishop et al. 2021a), but inferences of total limb muscle force-generating capacity provides a step closer toward achieving this goal.

Acknowledgements

T. French (Massachusetts Division of Fisheries and Wildlife) and R. Reed (United States Geological Survey, Daniel Beard Center) are thanked for providing the opossum and tegu specimens dissected here; P. Bergmann, C. Clemente, S. Cox, M. Martin and J. Rubenson are thanked for providing the original architectural data from their prior studies; and J. Hughes is

thanked for logistical assistance with dissections. The constructive comments of two anonymous reviewers, and the editor, on a prior version of the manuscript are also greatly appreciated.

Author contributions

P.J.B. and S.E.P. conceived the study design; P.J.B. collected anatomical data; P.J.B. and M.A.W. conducted statistical analyses and initial interpretations; all authors contributed to final interpretations and manuscript writing.

References

Alexander RM. 1977. Allometry of the limbs of antelopes (Bovidae). *Journal of Zoology* 183:125-146.

Alexander RM, Jayes AS, Maloiy GMO, and Wathuta EM. 1981. Allometry of the leg muscles of mammals. *Journal of Zoology* 194:539-552.

Allen V, Elsey RM, Jones N, Wright J, and Hutchinson JR. 2010. Functional specialization and ontogenetic scaling of limb anatomy in *Alligator mississippiensis*. *Journal of Anatomy* 216:423-445.

Allen V, Molnar J, Parker W, Pollard A, Nolan G, and Hutchinson JR. 2015. Comparative architectural properties of limb muscles in Crocodylidae and Alligatoridae and their relevance to divergent use of asymmetrical gaits in extant Crocodylia. *Journal of Anatomy* 225:569-582.

Bates KT, and Falkingham PL. 2018. The importance of muscle architecture in biomechanical reconstructions of extinct animals: a case study using *Tyrannosaurus rex*. *Journal of Anatomy* 233:625-635.

Bates KT, and Schachner ER. 2012. Disparity and convergence in bipedal archosaur locomotion. *Journal of the Royal Society Interface* 9:1339-1353.

Bennett MB. 1996. Allometry of the leg muscles of birds. *Journal of Zoology* 238:435-443.

Bennett MB, and Taylor GC. 1995. Scaling of elastic strain energy in kangaroos and the benefits of being big. *Nature* 378:56-59.

Bergmann PJ, and Hare-Drubka M. 2015. Hindlimb muscle anatomical mechanical advantage differs among joints and stride phases in basilisk lizards. *Zoology* 118:291-298.

Biewener AA. 1989. Scaling Body Support in Mammals: Limb Posture and Muscle Mechanics. *Science* 245:45-48.

Biewener AA. 2005. Biomechanical consequences of scaling. *Journal of Experimental Biology* 208:1665-1676.

Biewener AA, and Full RJ. 1992. Force platform and kinematic analysis. In: Biewener AA, ed. *Biomechanics – Structures and Systems: A Practical Approach*. New York: Oxford University Press, 45-73.

Bishop PJ. 2015. A critical re-evaluation of the hindlimb myology of moa (Aves: Dinornithiformes). *Memoirs of the Queensland Museum* 59:187-246.

Bishop PJ, Cuff AR, and Hutchinson JR. 2021a. How to build a dinosaur: musculoskeletal modelling and simulation of locomotor biomechanics in extinct animals. *Paleobiology* 47:1-38. 10.1017/pab.2020.46

Bishop PJ, Graham DF, Lamas LP, Hutchinson JR, Rubenson J, Hancock JA, Wilson RS, Hocknull SA, Barrett RS, Lloyd DG, and Clemente CJ. 2018. The Influence of Speed and Size on Avian Terrestrial Locomotor Biomechanics: Predicting Locomotion in Extinct Theropod Dinosaurs. *PLoS ONE* 13:e0192172.

Bishop PJ, Michel KB, Falisse A, Cuff AR, Allen VR, De Groote F, and Hutchinson JR. 2021b. Computational modelling of muscle fibre operating ranges in the hindlimb of a small ground bird (*Eudromia elegans*), with implications for modelling locomotion in extinct species. *PLOS Computational Biology* 17:1008843. 10.1371/journal.pcbi.1008843

Bodine SC, Roy RR, Meadows DA, Zernicke RF, Sacks RD, Fournier M, and Edgerton VR. 1982. Architectural, Histochemical, and Contractile Characteristics of a Unique Biarticular Muscle: the Cat Semitendinosus. *Journal of Neurophysiology* 48:192-201.

Böhmer C, Fabre A-C, Herbin M, Peigné S, and Herrel A. 2018. Anatomical Basis of Differences in Locomotor Behavior in Martens: A Comparison of the Forelimb Musculature Between Two Sympatric Species of *Martes*. *The Anatomical Record* 301:449-472.

Calow LJ, and Alexander RM. 1973. A mechanical analysis of a hind leg of a frog (*Rana temporaria*). *Journal of Zoology* 171:293-321.

Carlson KJ. 2006. Muscle architecture of the common chimpanzee (*Pan troglodytes*): perspectives for investigating chimpanzee behavior. *Primates* 47:218-229.

Carrano MT, and Hutchinson JR. 2002. Pelvic and hindlimb musculature of *Tyrannosaurus rex* (Dinosauria: Theropoda). *Journal of Morphology* 253:207-228.

Charles JP, Cappellari O, Spence AJ, Hutchinson JR, and Wells DJ. 2016. Musculoskeletal Geometry, Muscle Architecture and Functional Specialisations of the Mouse Hindlimb. *PLoS ONE* 11:e147669.

Cieri RL, Dick TJM, and Clemente CJ. 2020. Monitoring muscle over three orders of magnitude: widespread positive allometry among locomotor and body support musculature in the pectoral girdle of varanid lizards (Varanidae). *Journal of Anatomy* 237:1114-1135.

Cox SM, Easton KL, Lear MC, Marsh RL, Delp SL, and Rubenson J. 2019. The Interaction of Compliance and Activation on the Force-Length Operating Range and Force Generating Capacity of Skeletal Muscle: A Computational Study Using a Guinea Fowl Musculoskeletal Model. *Integrative and Comparative Biology*.

Cuff AR, Sparkes EL, Randau M, Pierce SE, Kitchener AC, Goswami A, and Hutchinson JR. 2016a. The scaling of postcranial muscles in cats (Felidae) I: forelimb, cervical, and thoracic muscles. *Journal of Anatomy* 229:128-141.

Cuff AR, Sparkes EL, Randau M, Pierce SE, Kitchener AC, Goswami A, and Hutchinson JR. 2016b. The scaling of postcranial muscles in cats (Felidae) II: hindlimb and lumbosacral muscles. *Journal of Anatomy* 229:142-152.

Currey JD. 2002. *Bones: Structure and Mechanics*. Princeton: Princeton University Press.

Dick TJM, and Clemente CJ. 2016. How to build your dragon: scaling of muscle architecture from the world's smallest to the world's largest monitor lizard. *Frontiers in Zoology* 13:8.

Dick TJM, and Clemente CJ. 2017. Where have All the Giants Gone? How Animals Deal with the Problem of Size. *PLOS Biology* 15:e2000473.

Ellis RG, Rankin JW, and Hutchinson JR. 2018. Limb Kinematics, Kinetics and Muscle Dynamics During the Sit-to-Stand Transition in Greyhounds. *Frontiers in Bioengineering and Biotechnology* 6:162.

Eng CM, Smallwood LH, Rainiero MP, Lahey M, Ward SR, and Lieber RL. 2008. Scaling of muscle architecture and fiber types in the rat hindlimb. *Journal of Experimental Biology* 211:2336-2345.

Etienne C, Houssaye A, and Hutchinson JR. 2021. Limb myology and muscle architecture of the Indian rhinoceros *Rhinoceros unicornis* and the white rhinoceros *Ceratotherium simum* (Mammalia: Rhinocerotidae). *PeerJ* 9:e11314.

826 Evans AR, Pollock TI, Cleuren SGC, Parker WMG, Richards HL, Garland KLS, Fitzgerald EMG, Wilson
827 TE, Hocking DP, and Adams JW. 2021. A universal power law for modelling the growth and
828 form of teeth, claws, horns, thorns, beaks, and shells. *BMC Biology* 19:58.
829 Fahn-Lai P, Biewener AA, and Pierce SE. 2020. Broad similarities in shoulder muscle architecture and
830 organization across two amniotes: implications for reconstructing non-mammalian synapsids.
831 *PeerJ* 8:8556.
832 Gans C, and Bock WJ. 1965. The functional significance of muscle architecture – a theoretical analysis.
833 *Ergebnisse der Anatomie und Entwicklungsgeschichte* 38.
834 Gatesy SM, and Biewener AA. 1991. Bipedal locomotion: effects of speed, size and limb posture in birds
835 and humans. *Journal of Zoology* 224:127-147.
836 Gaunt AS, and Gans C. 1992. Serially arranged myofibers: An unappreciated variant in muscle
837 architecture. *Experientia* 48:864-868.
838 Grand TI. 1977. Body Weight: Its Relation to Tissue Composition, Segment Distribution, and Motor
839 Function. I. Interspecific Comparisons. *American Journal of Physical Anthropology* 47:211-240.
840 Harmon LJ, Weir JT, Brock CD, Glor RE, and Challenger W. 2008. GEIGER: investigating evolutionary
841 radiations. *Bioinformatics* 24:129-131.
842 Hedges SB, Dudley J, and Kumar S. 2006. TimeTree: A public knowledge-base of divergence times
843 among organisms. *Bioinformatics* 22:2971-2972.
844 Hudson PE, Corr SA, Payne-Davis RC, Clancy SN, Lane E, and Wilson AM. 2011a. Functional anatomy
845 of the cheetah (*Acinonyx jubatus*) forelimb. *Journal of Anatomy* 218:375-385.
846 Hudson PE, Corr SA, Payne-Davis RC, Clancy SN, Lane E, and Wilson AM. 2011b. Functional anatomy
847 of the cheetah (*Acinonyx jubatus*) hindlimb. *Journal of Anatomy* 218:363-374.
848 Hutchinson JR. 2004. Biomechanical Modeling and Sensitivity Analysis of Bipedal Running Ability. I.
849 Extant Taxa. *Journal of Morphology* 262:421-440.
850 Hutchinson JR, Rankin JW, Rubenson J, Rosenbluth KH, Siston RA, and Delp SL. 2015. Musculoskeletal
851 modelling of an ostrich (*Struthio camelus*) pelvic limb: influence of limb orientation of muscular
852 capacity during locomotion. *PeerJ* 3:e1001.
853 Infantolino BW, Neuberger T, and Challis JH. 2012. The Arrangement of Fascicles in Whole Muscle. *The*
854 *Anatomical Record* 295:1174-1180.
855 Jenkins FA, Jr, and Weijs WA. 1979. The functional anatomy of the shoulder in the Virginia opossum
856 (*Didelphis virginiana*). *Journal of Zoology* 188:379-410.
857 Kikuchi, Y, and Kuraoka, A. 2014. Differences in muscle dimensional parameters btween non-formalin-
858 fixed (freeze-thawed) and formalin-fixed specimen in gorilla (*Gorilla gorilla*). *Mammal Study*
859 39:65-72.
860 Lamas LP, Main RP, and Hutchinson JR. 2014. Ontogenetic scaling patterns and functional anatomy of
861 the pelvic limb musculature in emus (*Dromaius novaehollandiae*). *PeerJ* 2:e716.
862 Lautenschlager S, Gill PG, Luo Z-X, Fagan MJ, and Rayfield EJ. 2018. The role of miniaturization in the
863 evolution of the mammalian jaw and middle ear. *Nature* 561:533-537.
864 Maloiy GMO, Alexander RM, Njau R, and Jayes AS. 1979. Allometry of the legs of running birds.
865 *Journal of Zoology* 187:161-167.
866 Martin ML, Travouillon KJ, Fleming PA, and Warburton NM. 2020. Review of the methods used for
867 calculating physiological cross-sectional area (PCSA) for ecological questions. *Journal of*
868 *Morphology* 281:778–789.
869 Martin ML, Warburton NM, Travouillon KJ, and Fleming PA. 2019. Mechanical similarity across
870 ontogeny of digging muscles in an Australian marsupial (*Isoodon fusciventer*). *Journal of*
871 *Morphology* 280:423-435.
872 McGowan CP, Skinner J, and Biewener AA. 2008. Hind limb scaling of kangaroos and wallabies
873 (superfamily Macropodoidea): implications for hopping performance, safety factor and elastic
874 savings. *Journal of Anatomy* 212:153-163.
875 Medler S. 2002. Comparative trends in shortening velocity and force production in skeletal muscle.
876 *American Journal of Physiology* 283:R368-R378.

Mendez J, and Keys A. 1960. Density and composition of mammalian muscle. *Metabolism – Clinical and Experimental* 9:184-188.
Moore AL, Budny JE, Russell AP, and Butcher MT. 2012. Architectural Specialization of the Intrinsic Thoracic Limb Musculature of the American Badger (*Taxidea taxus*). *Journal of Morphology* 274:35-48.
Ogihara N, Makishima H, Aoi S, Sugimoto Y, Tsuchiya K, and Nakatsukasa M. 2009. Development of an Anatomical Based Whole-Body Musculoskeletal Model of the Japanese Macaque (*Macaca fuscata*). *American Journal of Physical Anthropology* 139:323-338.
Olson RA, Glenn ZD, Cliffe RN, and Butcher MT. 2018. Architectural Properties of Sloth Forelimb Muscles (Pilosa: Bradypodidae). *Journal of Mammalian Evolution* 25:573-588.
Olson RA, Womble MD, Thomas DR, Glenn ZD, and Butcher MT. 2016. Functional Morphology of the Forelimb of the Nine-Banded Armadillo (*Dasypus novemcinctus*): Comparative Perspectives on the Myology of the Dasypodidae. *Journal of Mammalian Evolution* 23:49-69.
Orme D, Freckleton R, Thomas G, Petzoldt T, Fritz S, Isaac N, and Pearse W. 2018. caper: Comparative Analyses of Phylogenetics and Evolution in R.
Pagel M. 1999. Inferring the historical patterns of biological evolution. *Nature* 401.
Paxton H, Anthony NB, Corr SA, and Hutchinson JR. 2010. The effects of selective breeding on the architectural properties of the pelvic limb in broiler chickens: a comparative study across modern and ancestral populations. *Journal of Anatomy* 217:153-166.
Payne RC, Crompton RH, Isler K, Savage R, Vereecke EE, Günther MM, Thorpe SKS, and D'Août K. 2006. Morphological analysis of the hindlimb in apes and humans. I. Muscle architecture. *Journal of Anatomy* 208:709-724.
Payne RC, Hutchinson JR, Robilliard JJ, Smith NC, and Wilson AM. 2005. Functional specialisation of pelvic limb anatomy in horses (*Equus caballus*). *Journal of Anatomy* 206:557-574.
Pinheiro J, Bates D, DebRoy S, and Sarkar D. 2021. nlme: Linear and Nonlinear Mixed Effects Models.
Pollock CM, and Shadwick RE. 1994. Allometry of muscle, tendon, and elastic energy storage capacity in mammals. *American Journal of Physiology* 266:R1022-R1031.
Powell PL, Roy RR, Kanim P, Bello MA, and Edgerton VR. 1984. Predictability of skeletal muscle tension from architectural determinations in guinea pig hindlimbs. *Journal of Applied Physiology* 57:1715-1721.
R Core Team. 2021. *R: a language and environment for statistical computing*. Vienna: R Foundation for Statistical Computing.
Rajagopal A, Dembia CL, DeMers MS, Delp DD, Hicks JL, and Delp SL. 2016. Full-Body Musculoskeletal Model for Muscle-Driven Simulation of Human Gait. *IEEE Transactions of Biomedical Engineering* 63:2068-2079.
Regnault S, Fahn-Lai P, Norris RM, and Pierce SE. 2020. Shoulder Muscle Architecture in the Echidna (Monotremata: *Tachyglossus aculeatus*) Indicates Conserved Functional Properties. *Journal of Mammalian Evolution*. 10.1007/s10914-020-09498-6
Revell LJ. 2012. phytools: an R package for phylogenetic comparative biology (and other things). *Methods in Ecology and Evolution* 3:217-223.
Rose JA, Sandefur M, Huskey S, Demler JL, and Butcher MT. 2013. Muscle Architecture and Out-Force Potential of the Thoracic Limb in the Eastern Mole (*Scalopus aquaticus*). *Journal of Morphology* 274:1277-1287.
Rupert JE, Rose JA, Organ JM, and Butcher MT. 2015. Forelimb muscle architecture and myosin isoform composition in the groundhog (*Marmota monax*). *Journal of Experimental Biology* 218:194-205.
Sacks RD, and Roy RR. 1982. Architecture of the Hind Limb Muscles of Cats: Functional Significance. *Journal of Morphology* 173:185-195.
Schmidt-Nielsen K. 1985. *Scaling: Why is Animal Size So Important?* Cambridge: Cambridge University Press.
Sellers WI, Margetts L, Coria RA, and Manning PL. 2013. March of the Titans: The Locomotor Capabilities of Sauropod Dinosaurs. *PLoS ONE* 8:e78733.

928 Smaers JB, and Rohlf FJ. 2016. Testing species' deviation from allometric predictions using the
929 phylogenetic regression. *Evolution* 70:1145-1149.
930 Smith NC, Wilson AM, Jespers KJ, and Payne RC. 2006. Muscle architecture and functional anatomy of
931 the pelvic limb of the ostrich (*Struthio camelus*). *Journal of Anatomy* 209:765-779.
932 Smith RJ. 1980. Rethinking allometry. *Journal of Theoretical Biology* 87:97-111.
933 Sullivan SP, McGechie FR, Middleton KM, and Holliday CM. 2019. 3D Muscle Architecture of the
934 Pectoral Muscles of European Starling (*Sturnis vulgaris*). *Integrative Organismal Biology*
935 1:oby010.
936 Taylor GK, and Thomas ALR. 2014. *Evolutionary Biomechanics - Selection, Phylogeny, and Constraint*.
937 Oxford: Oxford University Press.
938 Vogel S. 2003. *Comparative Biomechanics: Life's Physical World*. Princeton: Princeton University Press.
939 Wareing K, Tickle PG, Stokkan K-A, Codd JR, and Sellers WI. 2011. The muscukoskeletal anatomy of
940 the reindeer (*Rangifer tarandus*): fore- and hindlimb. *Polar Biology* 34:1571-1578.
941 Williams SB, Payne RC, and Wilson AM. 2007a. Functional specialisation of the pelvic limb of the hare
942 (*Lepus europeus*). *Journal of Anatomy* 210:472-490.
943 Williams SB, Wilson AM, and Payne RC. 2007b. Functional specialisation of the thoracic limb of the
944 hare (*Lepus europeus*). *Journal of Anatomy* 210:491-505.
945 Williams SB, Wilson AM, Peckham K, and Payne RC. 2008. Functional anatomy and muscle moment
946 arms of the thoracic limb of an elite sprinting athlete: the racing greyhound (*Canis familiaris*).
947 *Journal of Anatomy* 213:373-382.
948 Wilson A, and Lichtwark G. 2011. The anatomical arrangement of muscle and tendon enhances limb
949 versatility and locomotor performance. *Philosophical Transactions of the Royal Society of*
950 *London, Series B* 366:1540-1553.
951 Witmer LM. 1995. The extant phylogenetic bracket and the importance of reconstructing soft tissues in
952 fossils. In: Thomason JJ, ed. *Functional Morphology in Vertebrate Paleontology*. Cambridge:
953 Cambridge University Press, 19-33.
954 Zajac FE. 1989. Muscle and tendon: properties, models, scaling, and application to biomechanics and
955 motor control. *Critical Reviews in Biomedical Engineering* 17:359-410.
956 Zihlman AL, McFarland RK, and Underwood CE. 2011. Functional Anatomy and Adaptation of Male
957 Gorillas (*Gorilla gorilla gorilla*) with Comparison to Male Orangutans (*Pongo pygmaeus*). *The*
958 *Anatomical Record* 294:1842-1855.

959
960
961
962
963
964
965
966
967
968
969
970
971

Figure captions

Figure 1. The requirements on muscles as part of a single, functionally integrated whole may impose constraints on their construction. (A) Changes in the size of one muscle may necessitate change in the size of adjacent muscle, such that total muscle volume (illustrated here in cross-section) may remain relatively constant. (B) Functional specialization of one muscle's architecture may necessitate concomitant changes to the architecture of other muscles, in order for a limb to remain capable of effectively executing a diverse range of tasks; total physiological cross-sectional area (PCSA) may therefore remain relatively constant. In this example, moving from left to right muscle 1 decreases PCSA but muscle 2 increases PCSA, such that total PCSA remains unaltered.

Figure 2. Total muscle mass v. body mass across extant terrestrial amniotes. This is shown for the forelimb and hindlimb, in terms of the limb as a whole, and parsed by proximal and distal compartments. Results are plotted on logarithmic coordinates, along with phylogenetic regression (pGLS) and 95% confidence intervals (CIs). Red = mammals, blue = reptiles, green = bipeds. Note the difference in vertical and horizontal scales. The slope expected under isometry is indicated in each case by the solid grey line, plotted clear of the data for ease of viewing. The slope and 95% CIs for each group are reported in each case, as are the sample sizes (in parentheses); also indicated are instances where a particular group exhibits statistically significant positive (⇧) or negative (⇩) allometry.

Figure 3. Mean size-normalized isometric strength v. body mass across extant terrestrial amniotes. Conventions as in Fig. 2. See Figs S2 and S3 for the results of median and total size-normalized isometric strength v. body mass.

Figure 4. Characteristic fibre length v. body mass across extant terrestrial amniotes. Conventions as in Fig. 2.

Figure 5. Total physiological cross-sectional area v. total muscle mass across extant terrestrial amniotes. Conventions as in Fig. 2.

Figure 1

The requirements on muscles as part of a single, functionally integrated whole may impose constraints on their construction.

(A) Changes in the size of one muscle may necessitate change in the size of adjacent muscle, such that total muscle volume (illustrated here in cross-section) may remain relatively constant. (B) Functional specialization of one muscle's architecture may necessitate concomitant changes to the architecture of other muscles, in order for a limb to remain capable of effectively executing a diverse range of tasks; total physiological cross-sectional area (PCSA) may therefore remain relatively constant. In this example, moving from left to right muscle 1 decreases PCSA but muscle 2 increases PCSA, such that total PCSA remains unaltered.

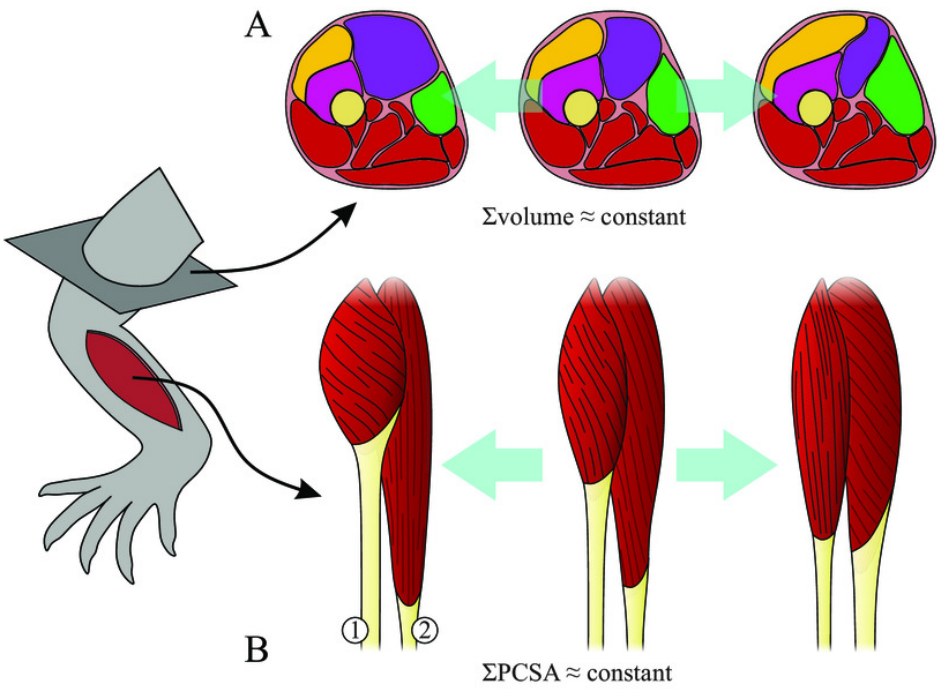
A
Σvolume ≈ constant
B
①
②
ΣPCSA ≈ constant

Figure 2

Total muscle mass v. body mass across extant terrestrial amniotes.

This is shown for the forelimb and hindlimb, in terms of the limb as a whole, and parsed by proximal and distal compartments. Results are plotted on logarithmic coordinates, along with phylogenetic regression (pGLS) and 95% confidence intervals (CIs). Red = mammals, blue = reptiles, green = bipeds. Note the difference in vertical and horizontal scales. The slope expected under isometry is indicated in each case by the solid grey line, plotted clear of the data for ease of viewing. The slope and 95% CIs for each group are reported in each case, as are the sample sizes (in parentheses); also indicated are instances where a particular group exhibits statistically significant positive (⇧) or negative (⇩) allometry.

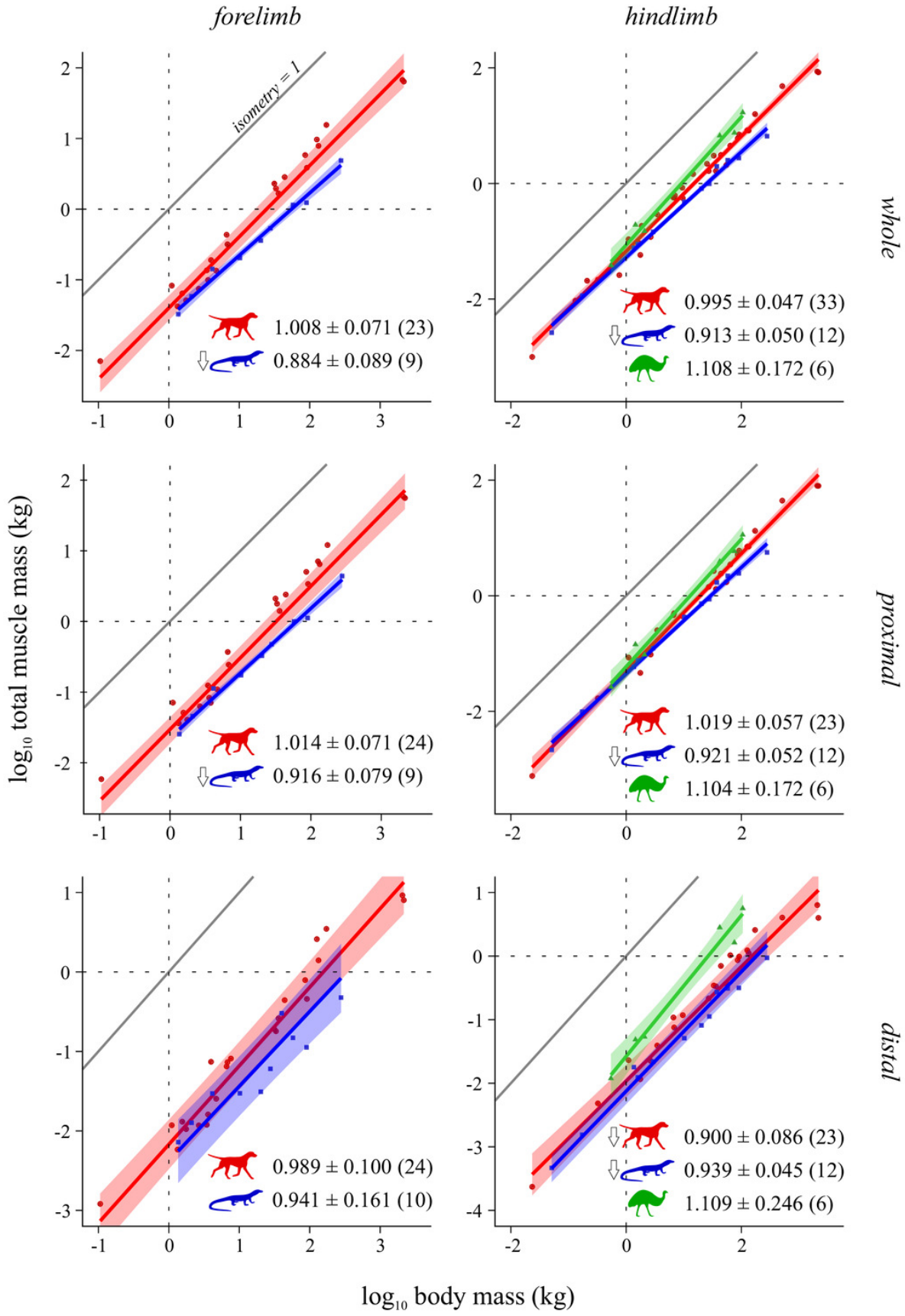
forelimb
hindlimb
whole
proximal
distal
isometry = 1
1.008 ± 0.071 (23)
0.884 ± 0.089 (9)
0.995 ± 0.047 (33)
0.913 ± 0.050 (12)
1.108 ± 0.172 (6)
1.014 ± 0.071 (24)
0.916 ± 0.079 (9)
1.019 ± 0.057 (23)
0.921 ± 0.052 (12)
1.104 ± 0.172 (6)
0.989 ± 0.100 (24)
0.941 ± 0.161 (10)
0.900 ± 0.086 (23)
0.939 ± 0.045 (12)
1.109 ± 0.246 (6)
log10 total muscle mass (kg)
log10 body mass (kg)

Figure 3

Mean size-normalized isometric strength v. body mass across extant terrestrial amniotes.

Conventions as in Fig. 2. See Figs S2 and S3 for the results of median and total size-normalized isometric strength *versus* body mass.

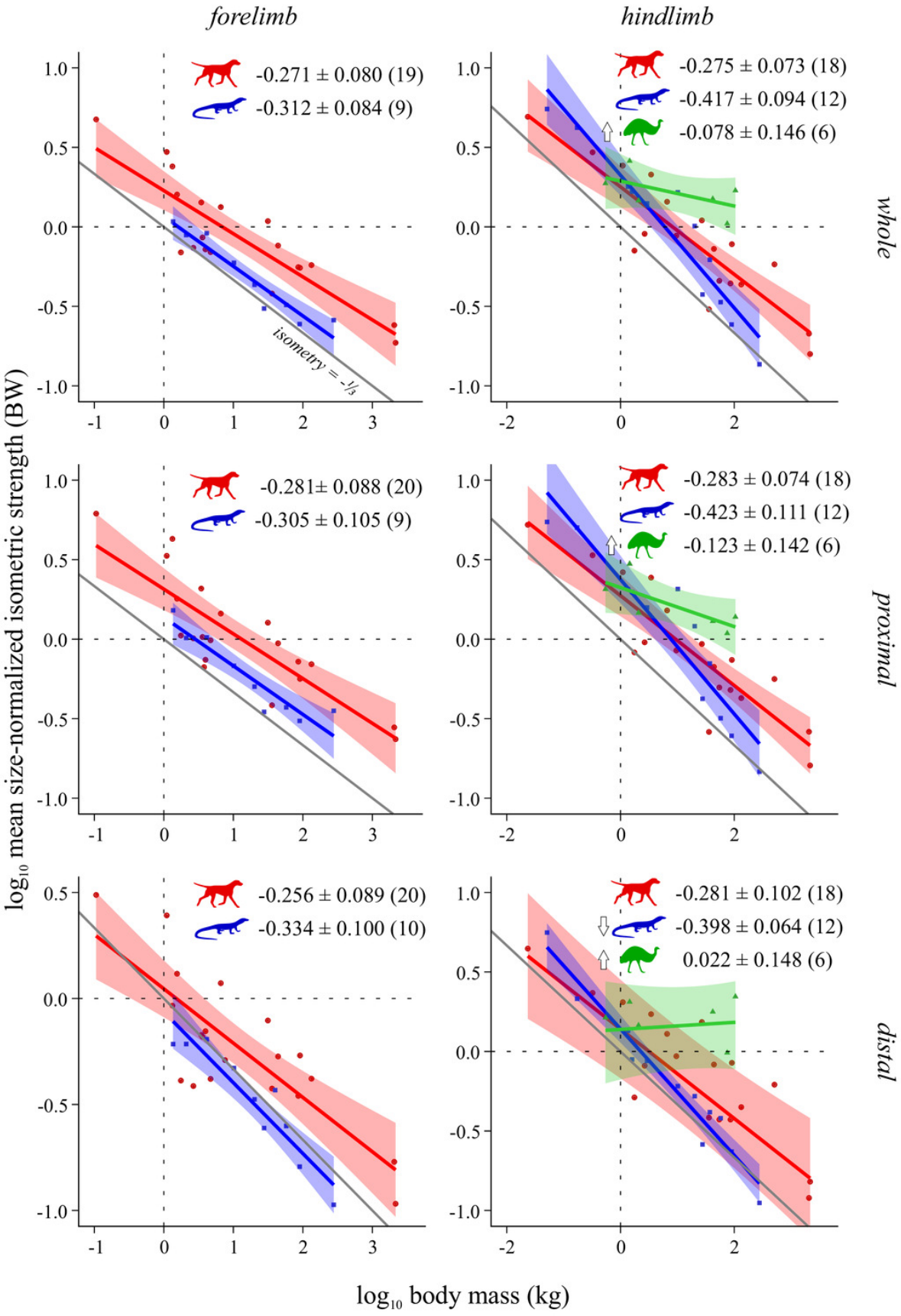
forelimb
hindlimb
whole
proximal
distal
-0.271 ± 0.080 (19)
-0.312 ± 0.084 (9)
isometry = -⅓
-0.275 ± 0.073 (18)
-0.417 ± 0.094 (12)
-0.078 ± 0.146 (6)
-0.281± 0.088 (20)
-0.305 ± 0.105 (9)
-0.283 ± 0.074 (18)
-0.423 ± 0.111 (12)
-0.123 ± 0.142 (6)
-0.256 ± 0.089 (20)
-0.334 ± 0.100 (10)
-0.281 ± 0.102 (18)
-0.398 ± 0.064 (12)
0.022 ± 0.148 (6)
log10 mean size-normalized isometric strength (BW)
log10 body mass (kg)

Figure 4

Characteristic fibre length v. body mass across extant terrestrial amniotes.

Conventions as in Fig. 2.

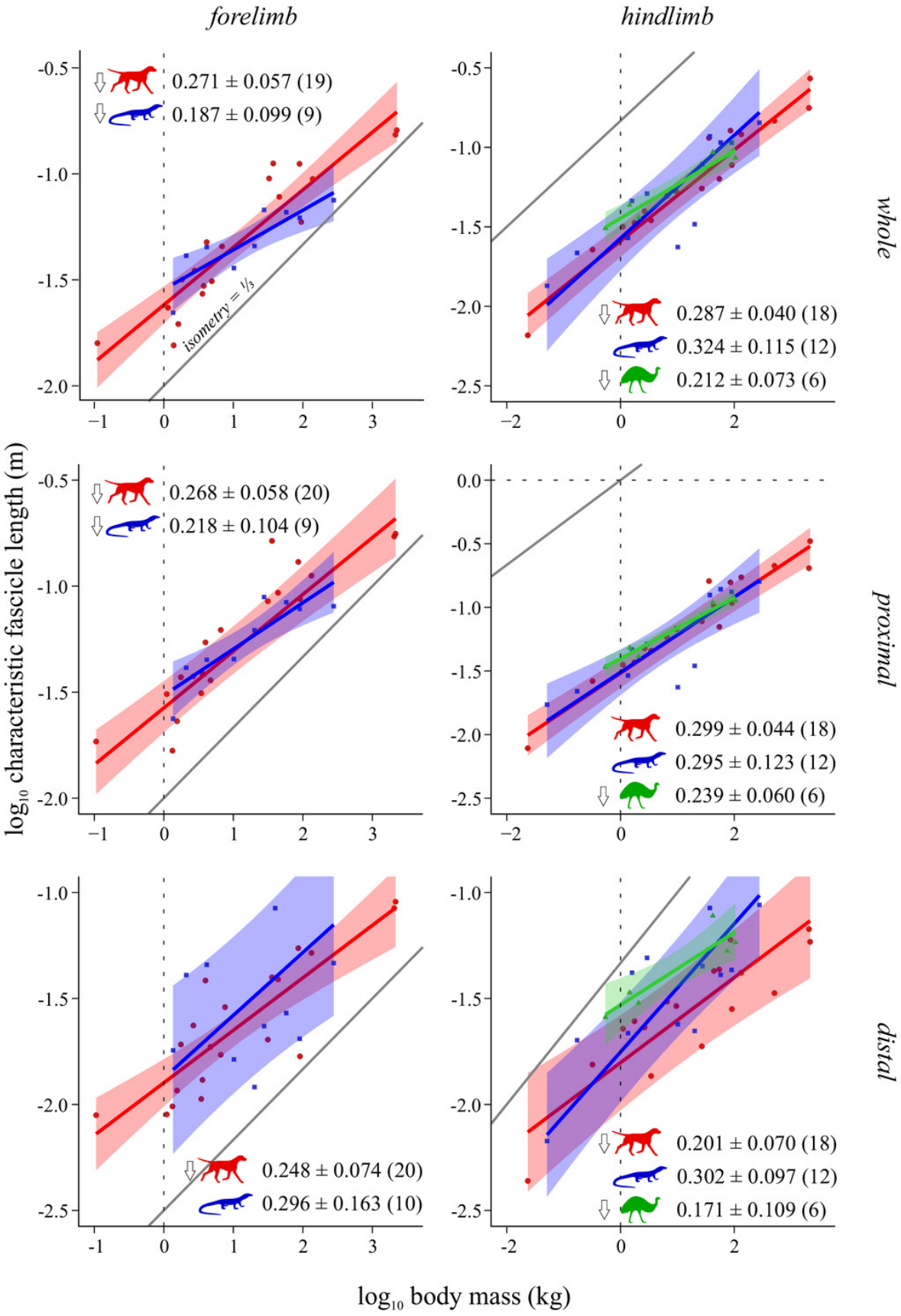
forelimb
hindlimb
whole
proximal
distal
0.271 ± 0.057 (19)
0.187 ± 0.099 (9)
isometry = ⅓
0.287 ± 0.040 (18)
0.324 ± 0.115 (12)
0.212 ± 0.073 (6)
0.268 ± 0.058 (20)
0.218 ± 0.104 (9)
0.299 ± 0.044 (18)
0.295 ± 0.123 (12)
0.239 ± 0.060 (6)
0.248 ± 0.074 (20)
0.296 ± 0.163 (10)
0.201 ± 0.070 (18)
0.302 ± 0.097 (12)
0.171 ± 0.109 (6)
log10 characteristic fascicle length (m)
log10 body mass (kg)

Figure 5

Total physiological cross-sectional area v. total muscle mass across extant terrestrial amniotes.

Conventions as in Fig. 2.

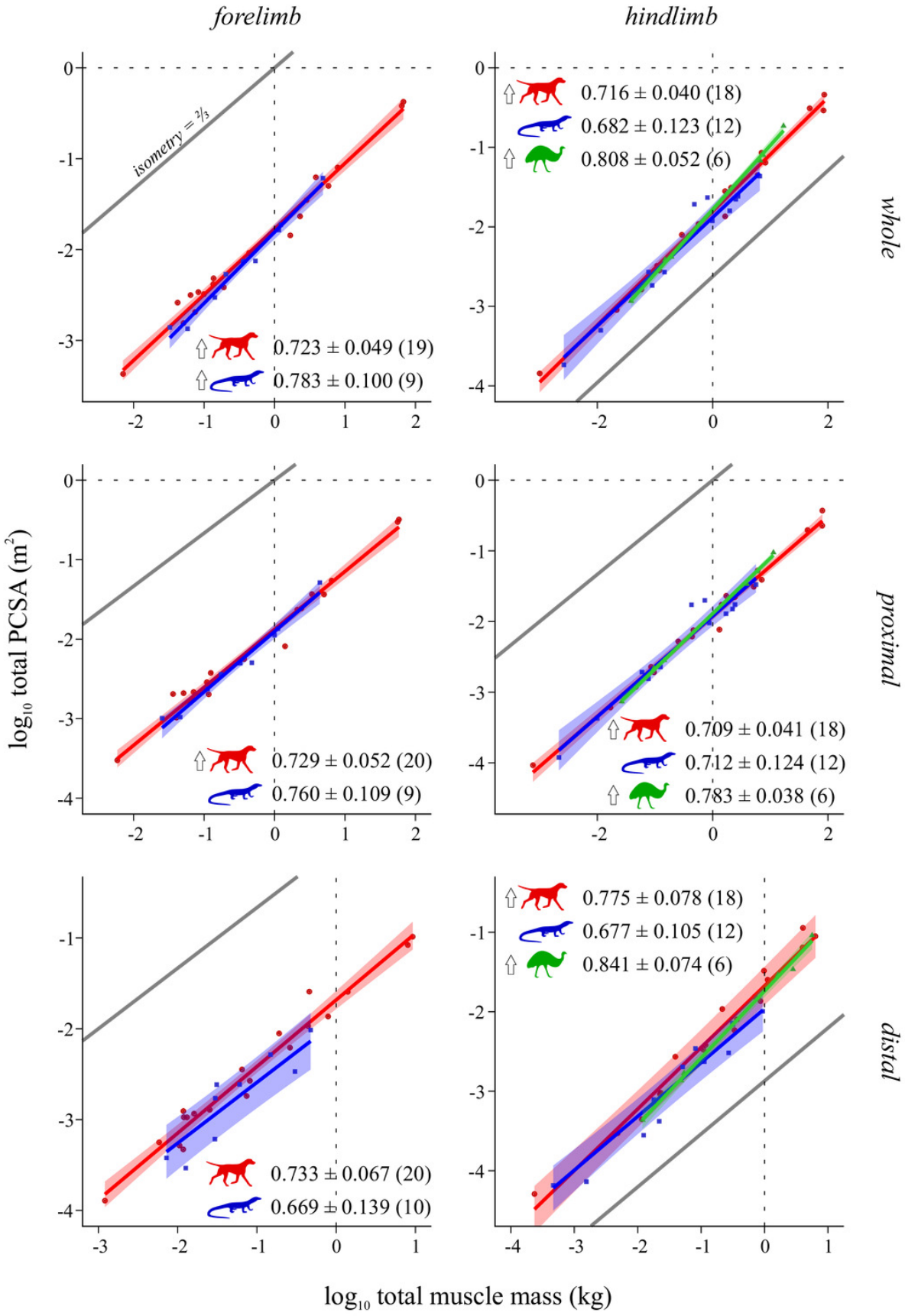
forelimb
hindlimb
whole
proximal
distal
isometry = 2/3
0.723 ± 0.049 (19)
0.783 ± 0.100 (9)
0.716 ± 0.040 (18)
0.682 ± 0.123 (12)
0.808 ± 0.052 (6)
0.729 ± 0.052 (20)
0.760 ± 0.109 (9)
0.709 ± 0.041 (18)
0.712 ± 0.124 (12)
0.783 ± 0.038 (6)
0.733 ± 0.067 (20)
0.669 ± 0.139 (10)
0.775 ± 0.078 (18)
0.677 ± 0.105 (12)
0.841 ± 0.074 (6)
log10 total PCSA (m2)
log10 total muscle mass (kg)

Table 1(on next page)

Summary of data sources used in the study.

List of species with architectural data for individual muscles, the major group they belong to (for the purposes of the statistical analyses conducted here), body mass, whether a given species contributed to the forelimb ('fore') or hindlimb ('hind') datasets, and studies in which the data were originally published. Note that birds and humans were analysed together in this study as 'bipeds'. See Table S1 for additional species and studies that contributed data on muscle mass only.

Table 1. Summary of data sources used in the study. List of species with architectural data for individual muscles, the major group they belong to (for the purposes of the statistical analyses conducted here), body mass, whether a given species contributed to the forelimb ('fore') or hindlimb ('hind') datasets, and studies in which the data were originally published. Note that birds and humans were analysed together in this study as 'bipeds'. See Table S1 for additional species and studies that contributed data on muscle mass only.

Species	Group	Body mass (kg)	Data	Study
Osteolaemus tetraspis	reptile	10.2	fore, hind	Allen et al. (2015)
Crocodylus johnstoni	reptile	20.19	fore, hind	Allen et al. (2015)
Crocodylus moreletii	reptile	27.7	fore, hind	Allen et al. (2015)
Alligator mississippiensis	reptile	57.7	fore, hind	Allen et al. (2015)
Melanosuchus niger	reptile	90	fore, hind	Allen et al. (2015)
Crocodylus niloticus	reptile	278	fore, hind	Allen et al. (2015)
Varanus tristis	reptile	0.173	hind	Dick & Clemente (2016)
Varanus varius	reptile	2.936	hind	Dick & Clemente (2016)
Varanus panoptes	reptile	4.15/1.6	fore, hind	Dick & Clemente (2016), Cieri et al. (2020)
Varanus komodoensis	reptile	40/37.3	fore, hind	Dick & Clemente (2016)
Varanus spenceri	reptile	2.098	fore	Cieri et al. (2020)
Salvator merianae	reptile	1.359	fore, hind	This study
Basiliscus vittatus	reptile	0.0511	hind	Bergmann & Hare-Drubka (2015)
Eudromia elegans	biped	0.545	hind	Bishop et al. (2021b)
Numida meleagris	biped	1.45	hind	Cox et al. (2019)
Gallus gallus (junglefowl)	biped	2.079	hind	Paxton et al. (2010)
Dromaius novaehollandiae	biped	42	hind	Lamas et al. (2014)
Struthio camelus	biped	105	hind	Smith et al. (2006)
Martes martes	mammal	1.55	fore	Böhmer et al. (2018)
Taxidea taxus	mammal	7.6	fore	Moore et al. (2012)
Canis familiaris	mammal	31.4/27	fore, hind	Williams et al. (2008), Ellis et al. (2018)
Felis nigripes	mammal	1.1	fore, hind	Cuff et al. (2016a),Cuff et al. (2016b)
Felis silvestris	mammal	2.66	fore, hind	Cuff et al. (2016a),Cuff et al. (2016b)
Leopardus pardalis	mammal	9.6	hind	Cuff et al. (2016b)
Caracal caracal	mammal	6.6	fore, hind	Cuff et al. (2016a),Cuff et al. (2016b)
Panthera uncia	mammal	36	fore, hind	Cuff et al. (2016a),Cuff et al. (2016b)
Panthera onca	mammal	44	fore, hind	Cuff et al. (2016a),Cuff et al. (2016b)
Panthera tigris	mammal	86	fore, hind	Cuff et al. (2016a),Cuff et al. (2016b)
Panthera leo	mammal	133	fore, hind	Cuff et al. (2016a),Cuff et al. (2016b)
Mus musculus	mammal	0.02345	hind	Charles et al. (2016)
Rattus norvegicus	mammal	0.323	hind	Eng et al. (2008)
Marmota monax	mammal	4.7	fore	Rupert et al. (2015)
Equus caballus	mammal	510	hind	Payne et al. (2005)
Ceratotherium simum	mammal	2160	fore, hind	Etienne et al. (2021)
Rhinoceros unicornis	mammal	2065	fore, hind	Etienne et al. (2021)
Lepus europeus	mammal	3.454	fore, hind	Williams et al. (2007a),Williams et al. (2007b)
Scalopus aquaticus	mammal	0.1062	fore	Rose et al. (2013)
Rangifer tarandus	mammal	91	fore, hind	Wareing et al. (2011)
Homo sapiens	biped	75.337	hind	Rajagopal et al. (2016)
Pan troglodytes	mammal	54.7	hind	Carlson (2006)
Bradypus variegatus	mammal	3.97	fore	Olson et al. (2018)
Dasypus novemcinctus	mammal	3.6	fore	Olson et al. (2016)
Isoodon fusciventer	mammal	1.329	fore	Martin et al. (2019)
Didelphis virginiana	mammal	1.759	fore, hind	This study
Tachyglossus aculeatus	mammal	3.79	fore	Regnault et al. (2020)

Table 2 (on next page)

Results of comparisons between each major group via pANCOVA, for the analysis of Σm_{muscle} v. m_{body}.

Each pairwise comparison was tested for differences in slope (S), intercept (I) and slope and intercept (S + I). Results for analyses without controlling for phylogeny are also presented (ANCOVA, †); significant results are in boldface; *df* = degrees of freedom.

Table 2. Results of comparisons between each major group via pANCOVA, for the analysis of Σm_{muscle} v. m_{body}. Each pairwise comparison was tested for differences in slope (S), intercept (I) and slope and intercept (S + I). Results for analyses without controlling for phylogeny are also presented (ANCOVA, †); significant results are in boldface; *df* = degrees of freedom.

anatomical region		test	mammals v. reptiles					mammals v. bipeds					reptiles v. bipeds				
			df	*F*	*P*	*F*†	*P*†	*df*	*F*	*P*	*F*†	*P*†	*df*	*F*	*P*	*F*†	*P*†
		S	2,29	1.442	0.24	32.465	**<0.001**										
	whole	I	2,29	1.639	0.211	33.14	**<0.001**										
		S + I	2,28	1.08	0.353	19.112	**<0.001**										
		S	2,30	1.008	0.324	25.295	**<0.001**										
forelimb	**proximal**	I	2,30	1.114	0.3	27.243	**<0.001**										
		S + I	2,29	0.73	0.491	14.967	**<0.001**										
		S	2,31	0.481	0.493	24.355	**<0.001**										
	distal	I	2,31	0.509	0.481	17.047	**<0.001**										
		S + I	2,30	0.377	0.689	11.945	**<0.001**										
		S	2,42	1.673	0.203	14.715	**<0.001**	2,36	5.181	**0.029**	11.763	**0.002**	2,15	21.811	**<0.001**	41.475	**<0.001**
	whole	I	2,42	0.259	0.613	13.985	**0.001**	2,36	2.616	0.115	10.143	**0.003**	2,15	8.332	**0.011**	32.61	**<0.001**
		S + I	2,41	0.855	0.433	9.291	**0.001**	2,35	2.519	0.095	6.554	**0.004**	2,14	13.11	**0.001**	36.147	**<0.001**
		S	2,32	4.268	**0.047**	16.724	**<0.001**	2,26	3.688	0.066	6.595	**0.016**	2,15	7.192	**0.017**	10.129	**0.006**
hindlimb	**proximal**	I	2,32	0.787	0.382	9.695	**0.004**	2,26	2.362	0.136	5.666	**0.025**	2,15	3.064	0.101	8.641	**0.01**
		S + I	2,31	2.112	0.138	8.643	**0.001**	2,25	1.831	0.181	3.564	**0.044**	2,14	3.521	0.058	5.825	**0.014**
		S	2,32	0.089	0.768	8.089	**0.008**	2,26	9.577	**0.005**	26.166	**<0.001**	2,15	10.088	**0.006**	15.239	**0.001**
	distal	I	2,32	0.199	0.659	15.57	**<0.001**	2,26	5.05	**0.033**	26.659	**<0.001**	2,15	6.737	**0.02**	31.079	**<0.001**
		S + I	2,31	0.166	0.848	7.819	**0.002**	2,25	4.64	**0.019**	17.517	**<0.001**	2,14	6.955	**0.008**	17.242	**<0.001**

Table 3(on next page)

Results of comparisons between each major group via pANCOVA and ANCOVA, for the analysis of mean F_{max}* v. m_{body}.

Conventions as per Table 2.

Table 3. Results of comparisons between each major group via pANCOVA and ANCOVA, for the analysis of mean F_{max}* v. m_{body}. Conventions as per Table 2.

anatomical region		test	mammals v. reptiles					mammals v. bipeds					reptiles v. bipeds				
			df	*F*	*P*	*F*†	*P*†	*df*	*F*	*P*	*F*†	*P*†	*df*	*F*	*P*	*F*†	*P*†
		S	2,25	1.212	0.282	9.013	**0.006**										
	whole	I	2,25	2.436	0.131	11.512	**0.002**										
		S + I	2,24	1.187	0.322	5.725	**0.009**										
		S	2,26	0.673	0.419	6.247	**0.019**										
forelimb	**proximal**	I	2,26	1.831	0.188	8.6	**0.007**										
		S + I	2,25	0.881	0.427	4.183	**0.027**										
		S	2,27	1.604	0.216	9.006	**0.006**										
	distal	I	2,27	1.554	0.223	8.939	**0.006**										
		S + I	2,26	0.942	0.403	4.824	**0.017**										
		S	2,27	6.699	**0.015**	6.699	**0.015**	2,21	14.358	**0.001**	14.358	**0.001**	2,15	35.374	**<0.001**	35.374	**<0.001**
	whole	I	2,27	0.886	0.355	0.886	0.355	2,21	6.785	**0.017**	6.785	**0.017**	2,15	6.387	**0.023**	6.387	**0.023**
		S + I	2,26	3.674	**0.039**	3.674	**0.039**	2,20	6.919	**0.005**	6.919	**0.005**	2,14	16.722	**<0.001**	16.722	**<0.001**
		S	2,27	4.379	**0.046**	4.379	**0.046**	2,21	10.455	**0.004**	10.455	**0.004**	2,15	19.785	**0.001**	19.785	**0.001**
hindlimb	**proximal**	I	2,27	0.238	0.629	0.238	0.629	2,21	5.882	**0.024**	5.882	**0.024**	2,15	4.273	0.056	4.273	0.056
		S + I	2,26	2.818	0.078	2.818	0.078	2,20	5.117	**0.016**	5.117	**0.016**	2,14	9.453	**0.003**	9.453	**0.003**
		S	2,27	2.232	0.147	12.439	**0.002**	2,21	11.022	**0.003**	14.949	**0.001**	2,15	49.529	**<0.001**	92.834	**<0.001**
	distal	I	2,27	0.096	0.76	7.245	**0.012**	2,21	3.055	0.095	6.169	**0.022**	2,15	3.88	0.068	16.093	**0.001**
		S + I	2,26	1.075	0.356	6.432	**0.005**	2,20	5.402	**0.013**	7.131	**0.005**	2,14	23.132	**<0.001**	47.383	**<0.001**

Table 4(on next page)

Results of comparisons between each major group via pANCOVA and ANCOVA, for the analysis of L^* v. m_{body}.

Conventions as per Table 2.

Table 4. Results of comparisons between each major group via pANCOVA and ANCOVA, for the analysis of L^* v. m_{body}.

Conventions as per Table 2.

anatomical region		test	mammals v. reptiles					mammals v. bipeds					reptiles v. bipeds				
			df	*F*	*P*	*F*†	*P*†	*df*	*F*	*P*	*F*†	*P*†	*df*	*F*	*P*	*F*†	*P*†
		S	2,25	1.537	0.227	1.537	0.227										
	whole	I	2,25	0.271	0.607	0.271	0.607										
		S + I	2,24	1.151	0.333	1.151	0.333										
		S	2,26	1.251	0.274	1.251	0.274										
forelimb	**proximal**	I	2,26	0.58	0.453	0.58	0.453										
		S + I	2,25	0.642	0.535	0.642	0.535										
		S	2,27	0.055	0.816	0.263	0.613										
	distal	I	2,27	0.113	0.74	0.288	0.596										
		S + I	2,26	0.062	0.94	1.921	0.167										
		S	2,27	0.395	0.535	0.025	0.875	2,21	0.379	0.545	0.073	0.789	2,15	0.603	0.45	0.013	0.91
	whole	I	2,27	0.181	0.674	0.157	0.695	2,21	0.651	0.429	1.437	0.244	2,15	0.114	0.741	0.243	0.629
		S + I	2,26	0.211	0.811	0.223	0.802	2,20	1.658	0.216	2.24	0.133	2,14	0.84	0.452	0.313	0.736
		S	2,27	0.002	0.964	0.794	0.381	2,21	0.269	0.609	0.175	0.68	2,15	0.041	0.842	0.094	0.764
hindlimb	**proximal**	I	2,27	0.008	0.929	0.367	0.55	2,21	0.273	0.607	0.372	0.548	2,15	0.346	0.565	0.636	0.438
		S + I	2,26	0.008	0.992	0.383	0.685	2,20	0.84	0.446	0.966	0.398	2,14	0.44	0.653	0.354	0.708
		S	2,27	3.644	0.067	2.953	0.097	2,21	0.64	0.433	3.941	0.06	2,15	1.323	0.268	0.14	0.713
	distal	I	2,27	0.277	0.603	5.02	**0.034**	2,21	1.846	0.189	11.95	**0.002**	2,15	0.422	0.526	1.106	0.31
		S + I	2,26	1.782	0.188	2.519	0.1	2,20	0.928	0.412	5.75	**0.011**	2,14	1.663	0.225	0.635	0.545

Table 5 (on next page)

Results of comparisons between each major group via pANCOVA and ANCOVA, for the analysis of ΣPCSA v. Σm_{muscle}.

Conventions as per Table 2.

Table 5. Results of comparisons between each major group via pANCOVA and ANCOVA, for the analysis of ΣPCSA v. Σm_{muscle}. Conventions as per Table 2.

anatomical region		test	mammals v. reptiles					mammals v. bipeds					reptiles v. bipeds				
			df	*F*	*P*	*F*†	*P*†	*df*	*F*	*P*	*F*†	*P*†	*df*	*F*	*P*	*F*†	*P*†
forelimb	whole	S	2,25	2.729	0.111	2.729	0.111										
		I	2,25	2.081	0.162	2.081	0.162										
		S + I	2,24	1.591	0.225	1.591	0.225										
	proximal	S	2,26	0.937	0.342	0.937	0.342										
		I	2,26	0.901	0.351	0.901	0.351										
		S + I	2,25	0.572	0.572	0.572	0.572										
	distal	S	2,27	0.01	0.92	3.383	0.077										
		I	2,27	0.689	0.414	3.327	0.079										
		S + I	2,26	0.434	0.653	1.726	0.198										
hindlimb	whole	S	2,27	0.075	0.787	0.075	0.787	2,21	5.272	**0.032**	5.272	0.032	2,15	1.215	0.288	1.215	0.288
		I	2,27	1.265	0.271	1.265	0.271	2,21	0.225	0.64	0.225	0.64	2,15	0.642	0.435	0.642	0.435
		S + I	2,26	0.611	0.551	0.611	0.551	2,20	2.676	0.093	2.676	0.093	2,14	1.124	0.353	1.124	0.353
	proximal	S	2,27	0.004	0.951	0.004	0.951	2,21	2.84	0.107	2.84	0.107	2,15	0.655	0.431	0.655	0.431
		I	2,27	1×10^{-4}	0.993	1×10^{-4}	0.993	2,21	0.313	0.582	0.313	0.582	2,15	0.028	0.869	0.028	0.869
		S + I	2,26	0.002	0.998	0.002	0.998	2,20	1.743	0.201	1.743	0.201	2,14	0.392	0.683	0.392	0.683
	distal	S	2,27	1.466	0.237	3.118	0.089	2,21	1.027	0.323	2.911	0.103	2,15	4.137	0.06	0.146	0.708
		I	2,27	0.505	0.483	9.851	**0.004**	2,21	0.195	0.663	3.387	0.08	2,15	0.233	0.636	0.738	0.404
		S + I	2,26	1.628	0.216	4.994	**0.015**	2,20	0.551	0.585	2.141	0.144	2,14	3.242	0.07	1.062	0.372

Table 6(on next page)

Pan-amniote regression (pGLS) coefficients for each comparison.

These are reported for data on a log10 scale; also reported is the mean percent prediction error (%PE), expressed in original (antilog) terms. Results for hindlimb analyses where the caudofemoralis longus was excluded from the reptile dataset are reported in Table S10.

Table 6. Pan-amniote regression (pGLS) coefficients for each comparison. These are reported for data on a log10 scale; also reported is the mean percent prediction error (%PE), expressed in original (antilog) terms. Results for hindlimb analyses where the caudofemoralis longus was excluded from the reptile dataset are reported in Table S10.

comparison	slope under isometry	limb	whole limb			proximal			distal		
			slope	intercept	mean %PE	slope	intercept	mean %PE	slope	intercept	mean %PE
Σm_{muscle} v. m_{body}	1.0	fore	1.0009	-1.5459	64.8	1.0076	-1.6512	66.52	0.9786	-2.3141	83.01
		hind	0.9798	-1.2764	40.77	0.9975	-1.3619	32.84	0.9069	-2.0589	55.32
mean F_{max}* v. m_{body}	-0.333	fore	-0.2798	0.1213	43.11	-0.2871	0.2092	46.12	-0.276	-0.0573	45.03
		hind	-0.3177	0.2791	33.58	-0.3266	0.3149	35.28	-0.3046	0.1345	45.66
median F_{max}* v. m_{body}	-0.333	fore	-0.3045	-0.0375	38.71	-0.3174	0.0782	44.67	-0.282	-0.1878	46.31
		hind	-0.2916	0.0154	40.38	-0.2757	0.0449	44.48	-0.3027	-0.0581	42.02
ΣF_{max}* v. m_{body}	-0.333	fore	-0.2896	1.5756	48.65	-0.2755	1.4068	48.2	-0.3146	1.0427	66.34
		hind	-0.307	1.7461	40.79	-0.2988	1.6095	36.11	-0.3314	1.1473	67.41
L* v. m_{body}	0.333	fore	0.2559	-1.6124	23.32	0.2603	-1.5407	21.54	0.2607	-1.8702	41.57
		hind	0.2943	-1.5699	21.46	0.3016	-1.5117	21.91	0.2296	-1.7568	35.41
ΣPCSA v. Σm_{muscle}	0.666	fore	0.7344	-1.7894	18.82	0.735	-1.8876	18.46	0.7215	-1.7914	38.93
		hind	0.7141	-1.8341	26.48	0.7095	-1.9253	26.2	0.746	-1.795	36.97

17
18
19
20
21
22
23
24